symmetry

MDPI

Article

Large Deflection Analysis of Axially Symmetric Deformation of Prestressed Circular Membranes under Uniform Lateral Loads

Xue Li [1], Jun-Yi Sun [1,2,*], Zhi-Hang Zhao [1] and Xiao-Ting He [1,2]

[1] School of Civil Engineering, Chongqing University, Chongqing 400045, China; 20161602025t@cqu.edu.cn (X.L.); 20135542@cqu.edu.cn (Z.-H.Z.); hexiaoting@cqu.edu.cn (X.-T.H.)

[2] Key Laboratory of New Technology for Construction of Cities in Mountain Area (Chongqing University), Ministry of Education, Chongqing 400045, China

* Correspondence: sunjunyi@cqu.edu.cn; Tel.: +86-(0)23-65120720

Received: 9 July 2020; Accepted: 9 August 2020; Published: 11 August 2020

Abstract: In this study, the problem of axisymmetric deformation of peripherally fixed and uniformly laterally loaded circular membranes with arbitrary initial stress is solved analytically. This problem could be called the generalized Föppl–Hencky membrane problem as the case where the initial stress in the membrane is equal to zero is the well-known Föppl–Hencky membrane problem. The problem can be mathematically modeled only in terms of radial coordinate owing to its axial symmetry, and in the present work, it is reformulated by considering an arbitrary initial stress (tensile, compressive, or zero) and by simultaneously improving the out-of-plane equilibrium equation and geometric equation, while the formulation was previously considered to fail to improve the geometric equation. The power-series method is used to solve the reformulated boundary value problem, and a new and more refined analytic solution of the problem is presented. This solution is actually observed to be able to regress into the well-known Hencky solution of zero initial stress, allowing the considered initial stress to be zero. Moreover, the numerical example conducted shows that the obtained power-series solutions for stress and deflection converge very well, and have higher computational accuracy in comparison with the existing solutions.

Keywords: initial stress; circular membrane; large deflection; power-series method; closed-form solution

1. Introduction

Thin films as structural components or structures are essential in many applications [1–4]. The so-called circular membrane problem usually refers to the problem of axially symmetric deformation of an initially flat, peripherally fixed, laterally uniformly loaded, linearly elastic, circular isotropic membrane with or without tensile or compressive initial stress. It is actually the mechanical model abstract from practical structural problems. This problem could be called the generalized Föppl–Hencky membrane problem as the case where the initial stress in the membrane is equal to zero is the well-known Föppl–Hencky membrane problem [5]. The term "membrane" here should be understood as the so-called fully stretched plate in mechanics whose upper and lower surfaces, regardless of its thickness, are simultaneously stretched under lateral loads owing to being "peripherally fixed". The so-called initial stress refers to the stress before uniformly laterally loading, which is produced by stretching or compressing the initially flat circular elastic membrane in the direction of the plane in which the initially flat circular elastic membrane locates. Obviously, the initial stress before uniformly laterally loading will have an influence on the mechanical behaviour of the circular membrane under uniform lateral loads, and in comparison with the stress resultant under laterally loading, the greater the initial stress, the greater the influence.

The initial stress can very easily be present in practical issues. For instance, the residual stress is the stress in the film/substrate systems or thin film devices after fabrication, which can be either tensile or compressive, and is usually an important parameter affecting the reliability or performance of film/substrate systems or thin film devices [6–11]. Therefore, the residual stress will be the so-called initial stress if the film in the film/substrate systems or thin film devices is further subjected to lateral loads. The initially flat circular elastic membrane attached to a stiff ring at its perimeter is often used to make diaphragm devices [4,12], while the membrane could be so inappropriately stressed that the stress in the attached initially flat circular membrane deviates from that expected, resulting in the so-called residual stress. In fact, the change in temperature or humidity could relax or tighten the initially flat circular membrane attached to the stiff ring, as long as the temperature or humidity at this time is different from that at attaching [13]. Such a relaxing or tightening is actually also a residual stress. The residual stress in thin film devices, as an initial stress of the thin film working under lateral loading, will result in the deviation of the performance of devices from that expected. Moreover, the variations in the processing conditions such as method of etching, humidity, temperature, or the order of fabrication procedures could give rise to a compressive or tensile residual stress in the film/substrate systems fabricated [7,9,11]. Such a residual stress could result in the delamination between a substrate and its coating [10], thus losing the reliability of film/substrate systems. To increase the reliability and ensure expected performance, the measurement of the residual stress in film/substrate systems and thin film devices is often found to be necessary after fabrication. To this end, a variety of ways have been developed to measure the residual stress, such as the peeling method [14], diffraction technique [15,16], diffraction topography technique [17], two beam laser reflection technique [18], and vibrational technique [19,20]. Among these ways, the so-called pressurized blister or bulge test technique [21–27] could be modelled as a circular membrane problem with or without initial tensile or compressive stress. There would be no need for an advanced experimental setup to simultaneously monitor the change in pressure and in blister dimension, if the analytical solution of the circular membrane problem, that is, the relation between pressure and blister dimension, can be available. Therefore, the analytical solutions of the circular membrane problems often play an important role in the design of thin film devices and the characterization of mechanical properties such as the residual stress, Poisson's ratio, modulus of elasticity, and adhesion strength for film/substrate systems or thin film devices [28].

Hencky, the recognized German scientist, originally dealt with the circular membrane problems without arbitrary initial stress, and a power-series solution of the problem was presented with the bending related terms in the Föppl–von Kármán equations of large deflection of thin plates ignored [5]. Chien [29] and Alekseev [30] corrected a computational error in [5]. This problem is the so-called Föppl–Hencky membrane problem (well-known Hencky problem for short), and its solution is usually referred to as the well-known Hencky solution, which is often cited in some studies of related issues [31–37]. Sun et al. reformulated the well-known Hencky problem by giving up the so-called small rotation angle assumption of membranes and by improving the out-of-plane equilibrium equation, and presented a new closed-form solution of the problem [38]. Further, Sun et al. [39] reformulated the well-known Hencky problem with the out-of-plane equilibrium equation, geometric equation simultaneously improved, and presented a new refined closed-form solution. As for the case of circular membranes with initial compressive or tensile stress, based on the modification of elastic equations, Ku [40] presented an analysis of large deflection of circular elastic membranes with initial tension under uniformly distributed loads, and He et al. [41] presented an analytic solution of axisymmetrical deformation of prestressed circular membranes under uniformly laterally loading. However, Sun et al. pointed out that it is unreasonable to modify the elastic equations because the initial stress before uniformly laterally loading should not give rise to a change in the constitutive relationship of membrane materials. Therefore, Sun et al. resolved the problem with initial stress under uniformly laterally loading and presented a new power-series solution of the problem, that is, the so-called extended Hencky solution [42]. The closed-form solution that is presented in [42] can be

regressed to the well-known Hencky solution, allowing the initial stress to be zero, while the solutions presented in [40,41] cannot. Moreover, the closed-form solution without the initial stress and small rotation angle assumption, which is presented in [38], was extended further to suit the more general cases with initial tensile or compressive stress, achieving the synchronous characterization for the interface and surface of film/substrate systems with residual stress [43]. Owing to improving the out-of-plane equilibrium equation and considering the initial tensile or compressive stress, this solution should be the prestressed solution with the best computational accuracy at present, and it has been incorporated into the study on the contact problem between Föppl–Hencky membranes and rigid surfaces [44].

In this study, the computational accuracy of the solution was further improved by simultaneously improving the geometric equation, out-of-plane equilibrium equation, and by considering an arbitrary initial stress. In the following section, the problem of axisymmetric deformation of the circular elastic membrane with an arbitrary initial stress is reformulated, the resulting boundary value problem is solved using the power-series method, and a new refined closed-form power-series solution is finally presented. In Section 3, on the basis of the numerical examples conducted, some important issues are discussed, such as the regression, convergence, effectiveness of the improved solution, and the effect of the initial stress on the obtained solution. Concluding remarks are presented in Section 4.

2. Membrane Equations and Closed-Form Solution

2.1. Reformulation of the Generalized Föppl–Hencky Membrane Problem

Suppose that, an initially flat, rotationally symmetric, linearly elastic unstretched circular membrane with Poisson's ratio v, Young's modulus of elasticity E, radius a, and thickness h is extended or shrunk a radial plane displacement u_0 at the periphery of radius a, and is then fixed at the radius a. A structure of the circular elastic membrane with an initial tensile or compressive stress is thus modelled. A uniformly-distributed transverse load q is applied quasi-statically onto the membrane surface, as depicted in Figure 1, where r and w denote the radial and transverse coordinates in the cylindrical coordinate system (r, φ, w) (w also denotes the transverse displacement of the deflected membrane), and the polar coordinate plane (r, φ) is arranged in the plane in which the geometric middle plane of the initially flat circular elastic membrane is located.

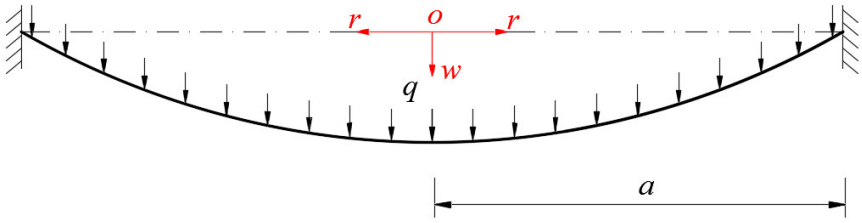

Figure 1. Geometry of the deformed circular membrane along a diameter $2a$ under load q.

Take a free body with radius $0 \le r \le a$ from the central portion of the deformed circular membrane, in order to study the static equilibrium problem of this free body under the joint actions of the uniformly-distributed loads q within r and the total force $2\pi r\sigma_r h$, which is produced by the membrane force $\sigma_r h$ acting on the boundary r, as depicted in Figure 2, where σ_r is the radial stress and θ is the slope angle of the deformed circular membrane.

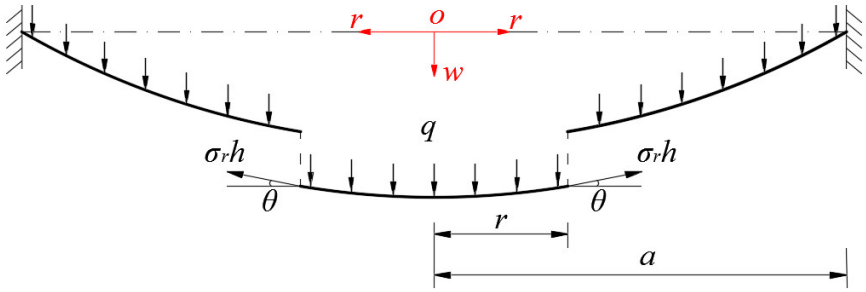

Figure 2. The free body diagram of the deformed circular membrane with radius $0 < r \leq a$.

Obviously, there are two forces in the vertical direction, that is, $\pi r^2 q$ (the total force of the uniformly-distributed loads q) and $2\pi r\sigma_r h \sin\theta$ (the total vertical membrane force which is produced by the membrane force $\sigma_r h$). So, the so-called out-of-plane equation of equilibrium [31,36,38,42] is

$$2\pi r\sigma_r h \sin\theta = \pi r^2 q, \tag{1}$$

where

$$\sin\theta = 1/\sqrt{1 + 1/\tan^2\theta} = 1/\sqrt{1 + 1/(-\mathrm{d}w/\mathrm{d}r)^2}. \tag{2}$$

Substituting Equation (2) into Equation (1), one has

$$\frac{1}{2} rq \sqrt{1 + 1/(\mathrm{d}w/\mathrm{d}r)^2} = \sigma_r h. \tag{3}$$

There are also two forces in the horizontal direction, the circumferential membrane force $\sigma_t h$ and the horizontal component of the membrane force $\sigma_r h$, where σ_t is the circumferential stress. So, the so-called in-plane equation of equilibrium may be written as

$$\frac{\mathrm{d}}{\mathrm{d}r}(r\sigma_r h) - \sigma_t h = 0. \tag{4}$$

Equation (4) can be found in any general theory of plates and shells, so it is not necessary to discuss its detailed derivation here. Suppose that the radial strain is denoted as e_r, the circumferential strain is denoted as e_t, the radial displacement is denoted as $u(r)$, and the transversal displacement is denoted as $w(r)$, then the so-called geometric equations [39] are

$$e_r = [(1 + \frac{\mathrm{d}u}{\mathrm{d}r})^2 + (\frac{\mathrm{d}w}{\mathrm{d}r})^2]^{1/2} - 1 \tag{5}$$

and

$$e_t = \frac{u}{r}. \tag{6}$$

Moreover, the stress and strain are still assumed to satisfy the linear elasticity relationship, so the so-called physical equations are

$$\sigma_r = \frac{E}{1-\nu^2}(e_r + \nu e_t) \tag{7}$$

and

$$\sigma_t = \frac{E}{1-\nu^2}(e_t + \nu e_r). \tag{8}$$

Eliminating e_r and e_t from Equations (5)–(8) yields

$$\sigma_r = \frac{E}{1-\nu^2}\{[(1 + \frac{\mathrm{d}u}{\mathrm{d}r})^2 + (\frac{\mathrm{d}w}{\mathrm{d}r})^2]^{1/2} - 1 + \nu\frac{u}{r}\} \tag{9}$$

and

$$\sigma_t = \frac{E}{1-\nu^2}\{\frac{u}{r} + \nu[(1+\frac{\mathrm{d}u}{\mathrm{d}r})^2 + (\frac{\mathrm{d}w}{\mathrm{d}r})^2]^{1/2} - v\}. \tag{10}$$

From Equations (4), (9) and (10), one has

$$\frac{u}{r} = \frac{1}{E}(\sigma_t - \nu\sigma_r) = \frac{1}{E}[\frac{\mathrm{d}}{\mathrm{d}r}(r\sigma_r) - v\sigma_r]. \tag{11}$$

After eliminating u from Equations (9) and (11), the usual so-called consistency equation can be written as

$$(\frac{1}{E}\sigma_r - \frac{v}{E}\sigma_t + 1)^2 - [\frac{1}{E}\frac{\mathrm{d}}{\mathrm{d}r}(r\sigma_t) - \frac{v}{E}\frac{\mathrm{d}}{\mathrm{d}r}(r\sigma_r) + 1]^2 - (\frac{\mathrm{d}w}{\mathrm{d}r})^2 = 0. \tag{12}$$

The boundary conditions to solve Equations (3), (4) and (12) can be determined based on the following solution to the plane stretching or compressing problem of the initially flat circular elastic membrane. In the problem of plane stretching or compressing (i.e., the initially flat circular elastic membrane is extended or shrunk to a radial plane displacement u_0 at $r = a$), $\mathrm{d}w/\mathrm{d}r = 0$. So, from Equations (5) and (6), one has

$$e_r = \frac{\mathrm{d}u}{\mathrm{d}r} \tag{13}$$

and

$$e_t = \frac{u}{r}. \tag{14}$$

Eliminating e_r and e_t from Equations (7), (8), (13) and (14) yields

$$\sigma_r = \frac{E}{1-\nu^2}(\frac{\mathrm{d}u}{\mathrm{d}r} + v\frac{u}{r}) \tag{15}$$

and

$$\sigma_t = \frac{E}{1-\nu^2}(\frac{u}{r} + v\frac{\mathrm{d}u}{\mathrm{d}r}). \tag{16}$$

From Equations (4), (15) and (16), one has

$$r^2\frac{\mathrm{d}^2u}{\mathrm{d}r^2} + r\frac{\mathrm{d}u}{\mathrm{d}r} - u = 0. \tag{17}$$

The boundary conditions to solve Equation (17) are

$$u = 0 \text{ at } r = 0 \tag{18}$$

and

$$u = u_0 \text{ at } r = a. \tag{19}$$

So, under the conditions of Equations (18) and (19), the solution of Equation (17) can be written as

$$\frac{u(r)}{r} = \frac{u_0}{a}. \tag{20}$$

From Equations (13)–(16) and (20), it is found that

$$e_r = e_t = e_0 = \frac{u_0}{a} \tag{21}$$

and

$$\sigma_r = \sigma_t = \sigma_0 = \frac{E}{1-v}\frac{u_0}{a}, \tag{22}$$

in which σ_0 denotes the so-called initial stress and e_0 denotes the initial strain. Equations (21) and (22) indicate that, for the problem of plane stretching or compressing, both stress and strain are two-axis

equal at every point on the flat circular membrane. This result is in accord with the fact that the residual stress is always uniform in film/substrate systems [9]. Therefore, the boundary conditions to solve Equations (3), (4) and (12) can finally be written as

$$\frac{\mathrm{d}w}{\mathrm{d}r} = 0 \text{ at } r = 0; \tag{23}$$

$$\frac{u}{r} = \frac{1}{E}(\sigma_t - v\sigma_r) = \frac{1}{E}[\frac{\mathrm{d}}{\mathrm{d}r}(r\sigma_r) - v\sigma_r] = \frac{u_0}{a} = \frac{1-v}{E}\sigma_0 \text{ at } r = a \tag{24}$$

and

$$w = 0 \text{ at } r = a. \tag{25}$$

2.2. Power Series Solution

The following dimensionless variables are used

$$Q = \frac{aq}{hE},\ W = \frac{w}{a},\ S_r = \frac{\sigma_r}{E},\ S_t = \frac{\sigma_t}{E},\ S_0 = \frac{\sigma_0}{E},\ x = \frac{r}{a}. \tag{26}$$

Transform Equations (3), (4), (12), (23)–(25) into

$$(4S_r^2 - x^2Q^2)(\frac{\mathrm{d}W}{\mathrm{d}x})^2 - x^2Q^2 = 0, \tag{27}$$

$$\frac{\mathrm{d}}{\mathrm{d}x}(xS_r) - S_t = 0, \tag{28}$$

$$(S_r - vS_t + 1)^2 - [\frac{\mathrm{d}}{\mathrm{d}x}(xS_t) - v\frac{\mathrm{d}}{\mathrm{d}x}(xS_r) + 1]^2 - (\frac{\mathrm{d}W}{\mathrm{d}x})^2 = 0, \tag{29}$$

$$\frac{\mathrm{d}W}{\mathrm{d}x} = 0 \text{ at } x = 0, \tag{30}$$

$$\frac{u}{r} = S_t - vS_r = \frac{\mathrm{d}}{\mathrm{d}x}(xS_r) - vS_r = S_0(1-v) \text{ at } x = 1 \tag{31}$$

and

$$W = 0 \text{ at } x = 1. \tag{32}$$

Eliminating $\mathrm{d}W/\mathrm{d}x$ and S_t from Equations (27)–(29), a nonlinear differential equation containing only variable S_r can be obtained

$$\begin{array}{c}(4S_r^2 - x^2Q^2)\{{S_r}^2 + 2S_r - 2(vS_r + 1)\frac{\mathrm{d}}{\mathrm{d}x}(xS_r) - (1-2v)[\frac{\mathrm{d}}{\mathrm{d}x}(xS_r)]^2 \\ -2x\frac{\mathrm{d}^2}{\mathrm{d}x^2}(xS_r) - 2(1-v)x\frac{\mathrm{d}}{\mathrm{d}x}(xS_r)\frac{\mathrm{d}^2}{\mathrm{d}x^2}(xS_r) - x^2[\frac{\mathrm{d}^2}{\mathrm{d}x^2}(xS_r)]^2\} - x^2Q^2 = 0\end{array}. \tag{33}$$

Given that the value of stress is finite at $x = 0$, then $S_r(x)$ can be expanded into the power-series of the x

$$S_r(x) = \sum_{i=0}^{\infty} b_i x^i. \tag{34}$$

After plugging Equation (34) into Equation (33), we obtain $b_i \equiv 0$ (i = 1, 3, 5, ...), and b_i (i = 2, 4, 6, ...) can be expressed in the polynomial about the undetermined constant b_0 (see Appendix A). While b_0 can be determined by the boundary condition at x = 1. From Equations (28) and (34), the condition of Equation (31) gives

$$\sum_{i=1}^{\infty} ib_i + (1-v)\sum_{i=0}^{\infty} b_i = S_0(1-v). \tag{35}$$

After substituting all expressions of b_i into Equation (35), an equation containing only b_0 can be obtained. So b_0 can be determined by solving this single variable equation, and the expression of S_r can thus be determined. As for S_t, with the known expression of S_r, it can easily be obtained from Equation (28), so it is not necessary to derive it here. Moreover, $W(x)$ can be expanded into the power-series of the x

$$W(x) = \sum_{i=0}^{\infty} c_i x^i. \tag{36}$$

Hence, after plugging Equations (34) and (36) into Equation (27), it is found that $c_i \equiv 0$ ($i = 1, 3, 5, \dots$), and c_i ($i = 2, 4, 6, \dots$) can be expressed into the polynomial about b_i (see Appendix B). The first coefficient c_0 is another undetermined constant, which can be determined by Equation (32). From Equation (36), Equation (32) gives

$$c_0 = -\sum_{i=1}^{\infty} c_i. \tag{37}$$

After substituting all expressions of c_i into Equation (37), the undetermined constant c_0 can be determined and, consequently, the expression of W can also be determined.

3. Results and Discussions

So far, the boundary condition Equation (23) or (30) has not been used yet. The following is the proof of whether the closed-form solution presented in Section 2 meets this boundary condition. The dimensional form of the deflection can be written as, from Equations (26) and (36),

$$w(r) = \sum_{i=0}^{\infty} \frac{c_i}{a^{i-1}} r^i. \tag{38}$$

The first derivative of Equation (38) is

$$\frac{\mathrm{d}w}{\mathrm{d}r} = \sum_{i=1}^{\infty} i \frac{c_i}{a^{i-1}} r^{i-1}. \tag{39}$$

So, $\mathrm{d}w/\mathrm{d}r = c_1$ at $r = 0$. Meanwhile, from the derivation in Section 2, it is already known that $c_1 \equiv 0$. Thus, $\mathrm{d}w/\mathrm{d}r \equiv 0$ at $r = 0$ because $c_1 \equiv 0$. This indicates that the boundary condition Equation (23) or (30) can be satisfied automatically, or in other words, the closed-form solution presented in Section 2 agrees with the physical characteristic of axially symmetric deformation of the circular membrane.

3.1. Regression of the Solution Presented in Second Section

The following is the proof of whether the analytic solution presented in Section 2 is able to be regressed to the well-known Hencky solution.

From Equation (26), it can be seen that when σ_0 is equal to zero, S_0 is also equal to zero. Hence, Equation (26) in [39] can easily be obtained by allowing S_0 in Equation (35) to be zero. This means that the analytic solution presented in Section 2, which applies to the case with initial stress, can be regressed to the solution presented in [39], which applies to the case without initial stress, because all the expressions for displacements and stresses obtained here have the same forms as those obtained in [39].

On the other hand, if the improved geometry equation (Equation (5) in [39] and this paper) is replaced by the classic geometric equation (Equation (5) in [38]), then the solution presented in [39] can be regressed to the solution presented in [38], which gives up the small rotation angle assumption and uses the classic geometric equation, but considers no initial stress.

Furthermore, if the small rotation angle assumption of membrane is still adopted, that is, replace Equation (2) in [38] by Equation (2) in [36], then the solution in [38] can be regressed into the well-known Hencky solution (which can be found in [5] or [36]).

Therefore, the analytic solution presented in Section 2 is able to be regressed into the well-known Hencky solution [5,36].

3.2. Comparison with Existing Solutions

For showing the difference between the existing solutions and the solution presented here, a numerical example was conducted, where four solutions were used, that is, the well-known Hencky solution that considers zero initial stress [5,36] and three solutions considering initial stress: the solution presented in this paper, the solution in [43], and the so-called extended Hencky solution in [42]. Suppose that a circular rubber thin film with Poisson's ratio $v = 0.47$, Young's modulus of elasticity $E = 7.84$ MPa, initial stress $\sigma_0 = 0.1$ MPa, and thickness $h = 0.2$ mm is fixed at radius $a = 20$ mm, and is then subjected to the transversely uniformly-distributed loads $q = 0.0001$ MPa, 0.003 MPa, and 0.01 MPa, respectively. Figure 3 shows the variations of the deflection w with the radial coordinate r and Figure 4 shows the variations of the radial stress σ_r with the radial coordinate r, where the solid lines represent the results calculated by the solution presented in this paper, which is denoted here as Solution 1; the dotted lines represent the results calculated by the solution in [43], which is denoted as Solution 2; the dotted-dashed lines represent the results calculated by the extended Hencky solution [42], which is denoted as Solution 3; and the dashed lines represent the results calculated by the well-known Hencky solution [5,36], which is denoted as Solution 4. The values of the maximum deflection w_m and maximum stress σ_m at $r = 0$ are listed in Table 1.

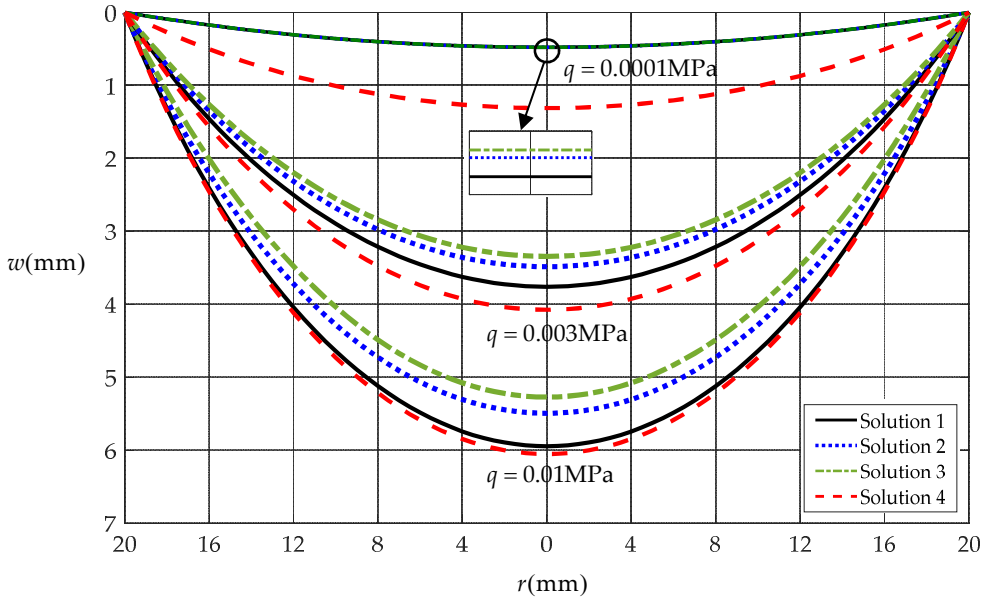

Figure 3. Variations of deflection w with r when σ_0 takes 0.1 MPa.

Table 1. The concrete values of w_m and σ_m when σ_0 takes 0.1 MPa.

	Loads q [MPa]	Solution 1	Solution 2	Solution 3	Solution 4
w_m [mm]	0.0001	0.47756	0.47743	0.47718	1.31183
	0.003	3.69050	3.43552	3.34403	4.07615
	0.01	5.94663	5.49420	5.27261	6.05366
σ_m [MPa]	0.0001	0.10536	0.10534	0.10534	0.04202
	0.003	0.44479	0.39752	0.36977	0.33981
	0.01	0.99162	0.86134	0.80763	0.78009

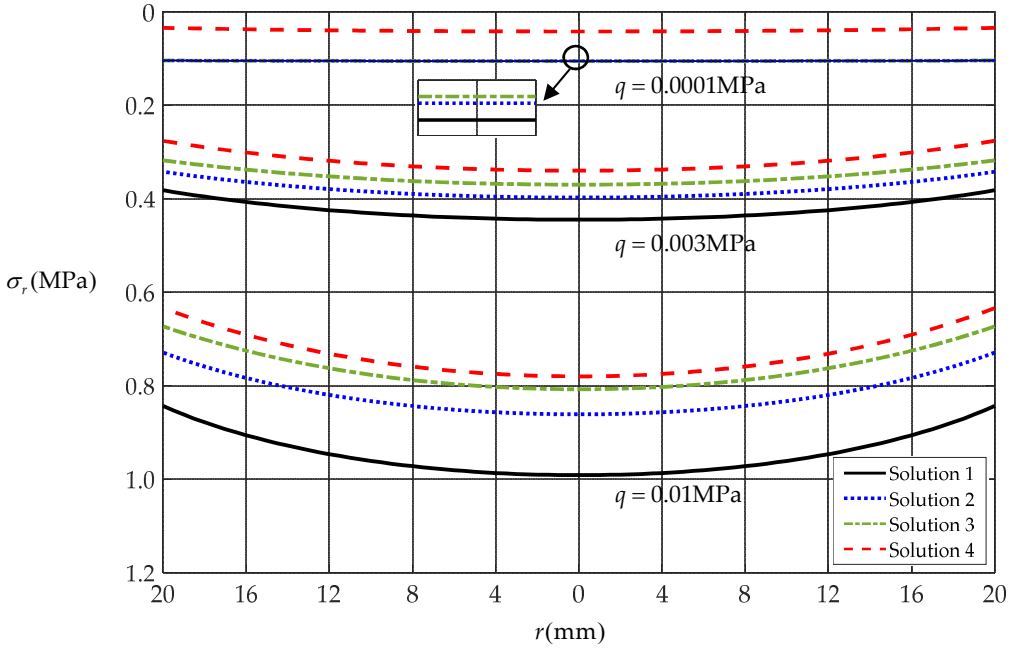

Figure 4. Variations of radial stress σ_r with r when σ_0 takes 0.1 MPa.

From Figures 3 and 4, it can be seen that the three solutions of considering initial stress (i.e., Solution 3, Solution 2, and Solution 1) agree quite closely for the loads q = 0.0001 MPa and diverge slowly as the loads intensify. This means that the improvements implemented in this paper have had an impact on the calculating precision of the solution, because Solution 3 is obtained using the classic geometric equation and classic out-of-plane equilibrium equation, Solution 2 is obtained using the classic geometric equation and improved out-of-plane equilibrium equation, while Solution 1 (i.e., the improved solution in this paper) is obtained using the improved geometric equation and improved out-of-plane equilibrium equation. The establishment of the classic out-of-plane equilibrium equation and geometric equation is based on the small rotation angle assumption of membrane, while the so-called "improved" here actually refers to giving up the small rotation angle assumption, resulting in a better adaptability of the solution to the rotation angle of membrane. From Figure 3, it can clearly be seen that, when the load q = 0.0001 MPa, the deflection calculated by Solution 4 (i.e., the well-known Hencky solution of considering zero initial stress) is far greater than the deflections calculated by Solution 3, Solution 2, and Solution 1, and when the load q = 0.003 MPa and 0.01 MPa, the deflection curve by Solution 4 slowly approaches the one by Solution 1 (the improved solution in this paper), and at the same time, it also slowly moves a little closer to the ones by Solution 3 and Solution 2, which may be seen from the data of Table 1. This is because the initial stress $\sigma_0 = 0.1$ MPa is considered by Solution 3, Solution 2, and Solution 1, while the initial stress $\sigma_0 = 0$ MPa is considered by Solution 4. Therefore, when the load q = 0.0001 MPa, the deflection calculated by Solution 4 is far greater than that by the three solutions considering $\sigma_0 = 0.1$ MPa, in other words, when the load q is relatively small, the initial stress of $\sigma_0 = 0.1$ MPa plays a main role in the deflection calculations by Solution 3, Solution 2, and Solution 1. Meanwhile, when the load q = 0.003 MPa and 0.01 MPa, the small rotation angle assumption, which is adopted in the classic out-of-plane equilibrium equation and geometric equation of the Solution 4, has relatively great influence on the deflection calculation by Solution 4, and the greater the load, the greater the influence. During the establishments of the out-of-plane equilibrium equation and geometric equation of the Solution 1, however, the small rotation angle assumption has been given up and thus has no influence on the deflection calculation by Solution 1. In other words, when the load q = 0.003 MPa and 0.01 MPa, the influence of the small rotation angle assumption on the deflection calculation by Solution 4 (the well-known Hencky solution) is far greater than the influence

of the initial stress of $\sigma_0 = 0.1$ MPa on the deflection calculation by Solution 1 (the improved solution in this paper).

On the other hand, Figures 3 and 4 also show that the applicable conditions or preconditions subject to compliance must be understood before using the solutions, or the used solution would not perform as well as expected, which could cause an unacceptable calculation error. For instance, from Table 1, it can be calculated that, when q takes 0.01 MPa and in comparison with Solution 1 (i.e., the improved solution in this paper), the error of the maximum deflection is about 7.61% for Solution 2 and about 11.34% for Solution 3, while the error of the maximum stress is about 13.14% for Solution 2 and about 18.56% for Solution 3. Such a large relative error is usually unacceptable in many practical technical problems, especially in the field of precision measurements such as the characterization of the mechanical properties of thin film/substrate systems [6–11]. Note that the allowable error for the precision measurement is usually less than 1%, for the instrument design is usually less than 3%, and for the civil engineering is usually less than 15%. In addition, it is conceivable that the relative error between the solution presented in this paper and the existing solutions will increase with the increase of the membrane deflection or applied loads. Therefore, in this sense, the improvement effect of this study on the analytical solution of the so-called generalized Föppl–Hencky membrane problem is obvious.

3.3. Convergence of the Power Series Solution Obtained in Second Section

The following is the proof of whether the power series solutions for $S_r(x)$ and $W(x)$ presented in Section 2 are convergent. However, only the special solutions for $S_r(x)$ and $W(x)$, rather than their general solutions, can be discussed, owing to the fact that the expressions of the coefficients b_i and c_i ($i = 2, 4, 6, \ldots$), which are expressed as the polynomial about the undetermined constants b_0 and c_0 (see Appendices A and B), are so intractable that the expressions of the remained terms of power-series solutions $S_r(x)$ and $W(x)$ cannot be obtained. It is already known, from the derivation in Section 2, that·the general solutions for $S_r(x)$ and $W(x)$ are the power-series of x (see Equations (34) and (36)), where $0 \le x \le 1$; b_i and c_i ($i = 2, 4, 6, \ldots$) are expressed as the polynomial about the coefficients b_0 and c_0; and for $i = 1,3,5, \ldots$, $b_i \equiv 0$ and $c_i \equiv 0$. It seems as if the special solutions for $S_r(x)$ and $W(x)$ can easily be obtained as long as the undetermined constants b_0 and c_0 can be determined by Equations (35) and (37). However, when solving a specific problem, only the partial sum of former n terms of Equations (34) and (36), rather than Equations (34) and (36), is substituted into Equations (31) and (32); otherwise, the resulting Equations (35) and (37) would contain two infinite series and are thus difficult to solve. Therefore, it may be seen that the determined values of b_0 and c_0 by Equations (35) and (37) depend on the value of terms n, and a different value of n will determine different values of b_0 and c_0. Hence, from this, it may be known that the special solution for $S_r(x)$ and $W(x)$ can be proved to be convergent by examining the variation of b_i and c_i with i for every value of terms n, especially examining the variation of b_0 and c_0 with terms n.

To this end, the numerical computations of b_0 and c_0 were started from $n = 4$, that is, started from the partial sum of former four terms for Equations (34) and (36), and the case of $q = 0.01$ MPa of the numerical example above was recalculated. Table 2 shows the obtained different numerical values of b_0 and b_i and the obtained values of c_0 and c_i are listed in Table 3. The variation of b_0 and c_0 with terms n is plotted in Figures 5 and 6, respectively, and the variation of b_i and c_i with i is, only for $n = 26$, shown in Figures 7 and 8, respectively. From Tables 2 and 3 or Figures 5 and 6, it is seen that the undetermined constants b_0 and c_0 converge reasonably well. From Tables 2 and 3 or Figures 7 and 8, it is seen that the coefficients b_i and c_i also converge reasonably well. Because $0 \le x \le 1$, it may thus be concluded that the special solutions for $S_r(x)$ and $W(x)$ are convergent. Furthermore, from Figures 5 and 6, it is also seen that, when $n = 20$, the undetermined constants b_0 and c_0 are already very close to their exact values. So, only the coefficients b_i and c_i ($i = 2,4,6, \ldots ,20$), which are expressed as the polynomial about b_0 and c_0, are shown in Appendices A and B, respectively.

Table 2. Values of b_0–b_6, b_8–b_{14}, b_{16}–b_{22}, and b_{24}–b_{26}.

n	b_0	b_2	b_4	b_6
4	1.20311×10^{-1}	-1.65094×10^{-2}	-3.36329×10^{-3}	—
6	1.23788×10^{-1}	-1.55680×10^{-2}	-2.95482×10^{-3}	-9.30349×10^{-4}
8	1.25201×10^{-1}	-1.52080×10^{-2}	-2.80646×10^{-3}	-8.58923×10^{-4}
10	1.25861×10^{-1}	-1.50439×10^{-2}	-2.74022×10^{-3}	-8.27699×10^{-4}
12	1.26198×10^{-1}	-1.49612×10^{-2}	-2.70718×10^{-3}	-8.12280×10^{-4}
14	1.26380×10^{-1}	-1.49168×10^{-2}	-2.68953×10^{-3}	-8.04083×10^{-4}
16	1.26483×10^{-1}	-1.48918×10^{-2}	-2.67964×10^{-3}	-7.99504×10^{-4}
18	1.26541×10^{-1}	-1.48776×10^{-2}	-2.67400×10^{-3}	-7.96896×10^{-4}
20	1.26579×10^{-1}	-1.48686×10^{-2}	-2.67044×10^{-3}	-7.95252×10^{-4}
22	1.26600×10^{-1}	-1.48635×10^{-2}	-2.66844×10^{-3}	-7.94329×10^{-4}
24	1.26607×10^{-1}	-1.48616×10^{-2}	-2.66770×10^{-3}	-7.93987×10^{-4}
26	1.26609×10^{-1}	-1.48612×10^{-2}	-2.66754×10^{-3}	-7.93915×10^{-4}
n	b_8	b_{10}	b_{12}	b_{14}
8	-3.27991×10^{-4}	—	—	—
10	-3.11944×10^{-4}	-1.33536×10^{-4}	—	—
12	-3.04098×10^{-4}	-1.29313×10^{-4}	-5.98144×10^{-5}	—
14	-2.99948×10^{-4}	-1.27091×10^{-4}	-5.85763×10^{-5}	-2.86800×10^{-5}
16	-2.97637×10^{-4}	-1.25857×10^{-4}	-5.78906×10^{-5}	-2.82872×10^{-5}
18	-2.96323×10^{-4}	-1.25157×10^{-4}	-5.75019×10^{-5}	-2.80649×10^{-5}
20	-2.95495×10^{-4}	-1.24716×10^{-4}	-5.72576×10^{-5}	-2.79253×10^{-5}
22	-2.95030×10^{-4}	-1.24469×10^{-4}	-5.71206×10^{-5}	-2.78471×10^{-5}
24	-2.94858×10^{-4}	-1.24377×10^{-4}	-5.70698×10^{-5}	-2.78181×10^{-5}
26	-2.94822×10^{-4}	-1.24358×10^{-4}	-5.70592×10^{-5}	-2.78121×10^{-5}
n	b_{16}	b_{18}	b_{20}	b_{22}
16	-1.44729×10^{-5}	—	—	—
18	-1.43427×10^{-5}	-7.60266×10^{-6}	—	—
20	-1.42610×10^{-5}	-7.55386×10^{-6}	-4.12285×10^{-6}	—
22	-1.42152×10^{-5}	-7.52654×10^{-6}	-4.10626×10^{-6}	-2.29738×10^{-6}
24	-1.41983×10^{-5}	-7.51642×10^{-6}	-4.10013×10^{-6}	-2.29360×10^{-6}
26	-1.41947×10^{-5}	-7.51431×10^{-6}	-4.09884×10^{-6}	-2.29281×10^{-6}
n	b_{24}	b_{26}		
24	-1.31103×10^{-6}	—	—	—
26	-1.31054×10^{-6}	-7.63614×10^{-7}	—	—

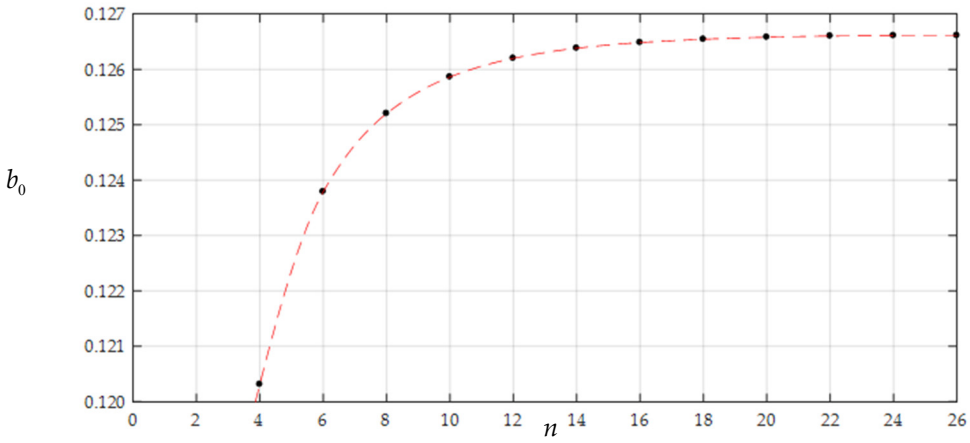

Figure 5. The variation of b_0 with n.

Table 3. Values of c_0–c_6, c_8–c_{14}, c_{16}–c_{22}, and c_{24}–c_{26}.

n	c_0	c_2	c_4	c_6
4	3.01849×10^{-1}	-2.65045×10^{-1}	-3.68042×10^{-2}	—
6	3.00567×10^{-1}	-2.575995×10^{-1}	-3.32919×10^{-2}	-9.97580×10^{-3}
8	2.99505×10^{-1}	-2.546935×10^{-1}	-3.19904×10^{-2}	-9.31291×10^{-3}
10	2.98554×10^{-1}	-2.53357×10^{-1}	-3.14045×10^{-2}	-9.02080×10^{-3}
12	2.97949×10^{-1}	-2.52681×10^{-1}	-3.11111×10^{-2}	-8.87599×10^{-3}
14	2.97569×10^{-1}	-2.52317×10^{-1}	-3.09540×10^{-2}	-8.79885×10^{-3}
16	2.97332×10^{-1}	-2.52112×10^{-1}	-3.08659×10^{-2}	-8.75572×10^{-3}
18	2.97207×10^{-1}	-2.51995×10^{-1}	-3.08156×10^{-2}	-8.73114×10^{-3}
20	2.97173×10^{-1}	-2.51921×10^{-1}	-3.07839×10^{-2}	-8.71564×10^{-3}
22	2.97171×10^{-1}	-2.51879×10^{-1}	-3.07661×10^{-2}	-8.70693×10^{-3}
24	2.97171×10^{-1}	-2.51864×10^{-1}	-3.07594×10^{-2}	-8.70370×10^{-3}
26	2.97171×10^{-1}	-2.51861×10^{-1}	-3.07581×10^{-2}	-8.70303×10^{-3}
n	c_8	c_{10}	c_{12}	c_{14}
8	-3.47991×10^{-3}	—	—	—
10	-3.35337×10^{-3}	-1.41877×10^{-3}	—	—
12	-3.27724×10^{-3}	-1.37720×10^{-3}	-6.26249×10^{-4}	—
14	-3.23690×10^{-3}	-1.35529×10^{-3}	-6.14040×10^{-4}	-2.93518×10^{-4}
16	-3.21441×10^{-3}	-1.34310×10^{-3}	-6.07272×10^{-4}	-2.89687×10^{-4}
18	-3.20161×10^{-3}	-1.33618×10^{-3}	-6.03433×10^{-4}	-2.87518×10^{-4}
20	-3.19355×10^{-3}	-1.33183×10^{-3}	-6.01020×10^{-4}	-2.86156×10^{-4}
22	-3.18902×10^{-3}	-1.32938×10^{-3}	-5.99666×10^{-4}	-2.85392×10^{-4}
24	-3.18734×10^{-3}	-1.32848×10^{-3}	-5.99164×10^{-4}	-2.85109×10^{-4}
26	-3.18699×10^{-3}	-1.32829×10^{-3}	-5.99059×10^{-4}	-2.85050×10^{-4}
n	c_{16}	c_{18}	c_{20}	c_{22}
16	-1.43691×10^{-4}	—	—	—
18	-1.42448×10^{-4}	-7.27170×10^{-5}	—	—
20	-1.41668×10^{-4}	-7.22652×10^{-5}	-3.77500×10^{-5}	—
22	-1.41231×10^{-4}	-7.20122×10^{-5}	-3.76022×10^{-5}	-2.00212×10^{-5}
24	-1.41069×10^{-4}	-7.19185×10^{-5}	-3.75475×10^{-5}	-1.99890×10^{-5}
26	-1.41035×10^{-4}	-7.18989×10^{-5}	-3.75361×10^{-5}	-1.99822×10^{-5}
n	c_{24}	c_{26}		
24	-1.08172×10^{-5}	—	—	—
26	-1.08132×10^{-5}	-5.93435×10^{-6}	—	—

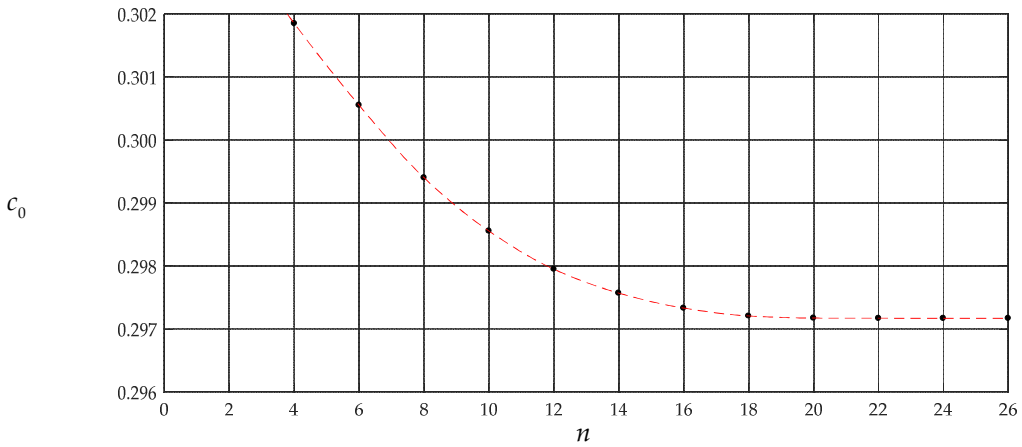

Figure 6. The variation of c_0 with n.

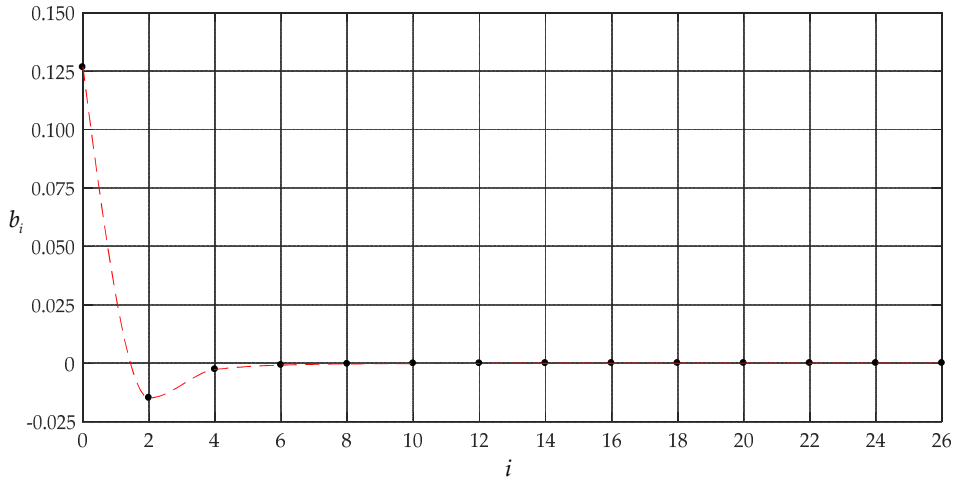

(**a**)

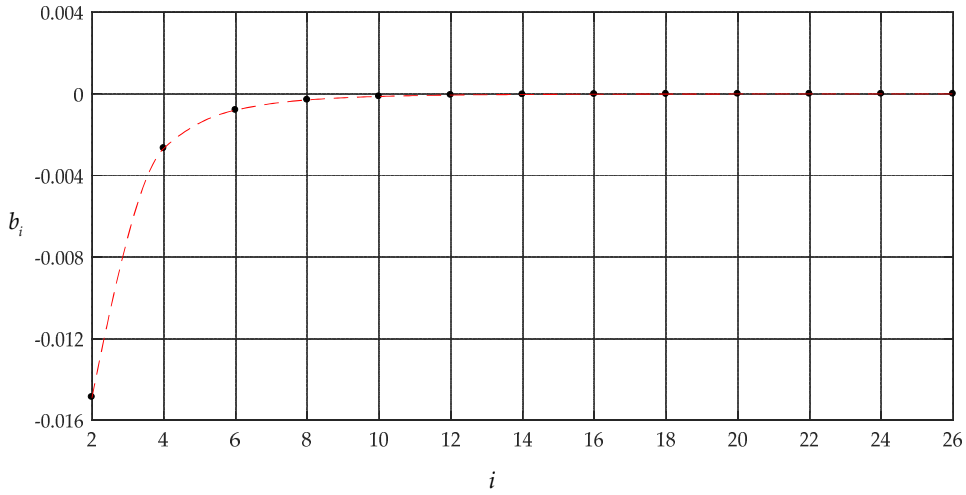

(**b**)

Figure 7. Distribution of b_i with i when $n = 26$: (**a**) $i = 0, 2, 4, 6, \ldots, 26$ and (**b**) $i = 2, 4, 6, \ldots, 26$.

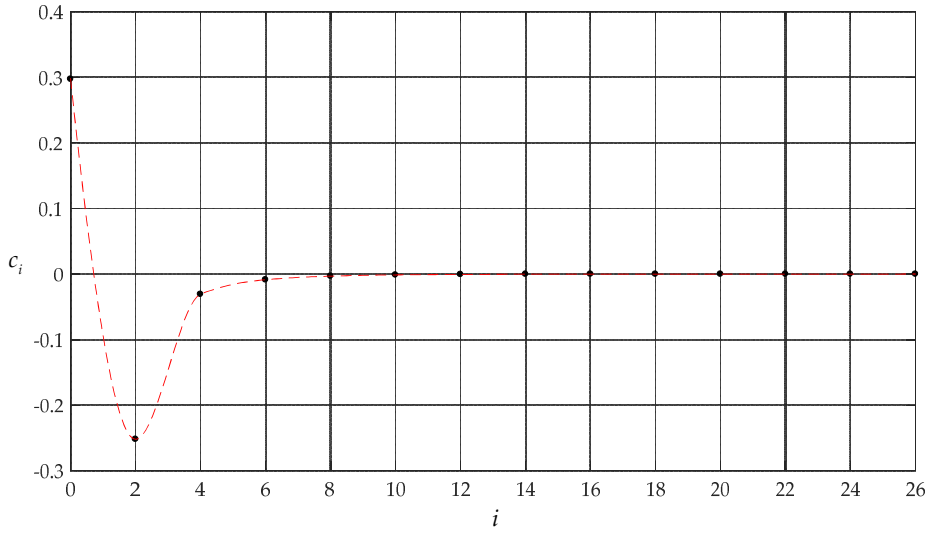

(**a**)

Figure 8. *Cont.*

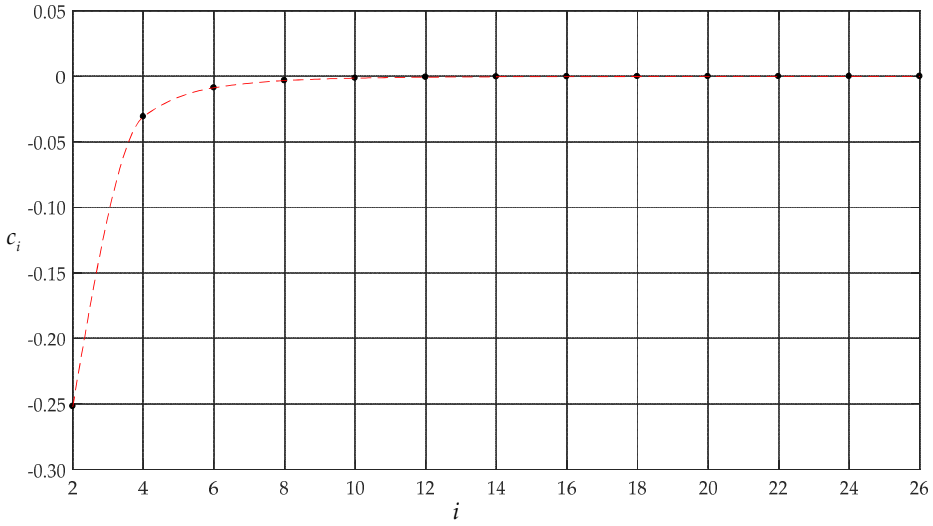

(**b**)

Figure 8. Distribution of c_i with i when $n = 26$: (**a**) $i = 0, 2, 4, 6, \ldots, 26$ and (**b**) $i = 2, 4, 6, \ldots, 26$.

4. Concluding Remarks

In this study, the well-known Hencky problem is generalized to include the case of an arbitrary initial compressive or tensile stress, where the classic geometric equation and out-of-plane equilibrium equation are simultaneously improved. The following conclusions can, from this study, be drawn.

In comparison with the existing solutions, which consider initial stress, the closed-form solution presented in this paper has a higher computational accuracy. The use of existing solutions does not bring too much computational error for the case of relatively small deflection of membranes, but for the relatively large deflection, the closed-form solution presented in this paper should be given priority. Otherwise, an unacceptable calculation error could be caused, which has, in the conducted numerical example, been shown to be 11.34% deflection error and 18.56% stress error. Meanwhile, the allowable error for the precision measurement, instrument design, and civil engineering is usually less than 1%, 3%, and 15%, respectively.

The proof of convergence of the power series solutions for $S_r(x)$ and $W(x)$ must be conducted, but only to their special solutions, rather than their general solutions, owing to the somewhat intractable forms of expression of the coefficients b_i and c_i (i = 2,4,6, ...), that is, the polynomial functions with regard to the undetermined constants b_0 and c_0(see Appendices A and B). Therefore, for the convergence proof of the special solutions for $S_r(x)$ and $W(x)$, the following two aspects should be given full attention. First, the numerical computation of the undetermined constants b_0 and c_0 has to be started from a smallest partial sum of the former n terms of the power series, usually n = 3 or 4. Then, with the help of a scatter plot, the saturation degree for the computed obtained numerical values of b_0 and c_0 can be examined. The saturation degree for the coefficients b_i and c_i is not examined until a satisfactory saturation degree for the computed obtained numerical values of b_0 and c_0 has been observed. A demonstrated example and the detailed operating steps may be found in Section 3.

The large deflection phenomenon of the membrane with initial compressive or tensile stress appears very easily, especially in the mechanical properties' characterization using the thin-film/substrate delamination by pressurized blister or bulge tests, where the maximum deflection of the blistering thin-film could reach half the radius of the circular blistering thin film, or even larger. The solutions in the existing literature are not suitable for such a large deflection owing to the approximations adopted in the classic out-of-plane equilibrium equation and geometric equation, while the solution presented in this paper has given up these approximations and can thus be used to calculate such a large deflection. Therefore, in this sense, the work presented in this paper should have a positive significance for these technical application fields.

Author Contributions: Conceptualization, J.-Y.S. and X.-T.H.; methodology, J.-Y.S. and X.L.; validation, X.-T.H.; writing—original draft preparation, Z.-H.Z. and X.L.; writing—review and editing, X.L. and X.-T.H.; visualization, X.L.; funding acquisition, J.-Y.S. All authors have read and agreed to the published version of the manuscript.

Funding: This research was funded by the National Natural Science Foundation of China (Grant No. 11772072).

Conflicts of Interest: The authors declare no conflict of interest.

Nomenclature

a	Radius of the circular membrane
h	Thickness of the circular membrane
E	Young's modulus of elasticity
v	Poisson's ratio
q	Uniformly distributed transverse loads
r	Radial coordinate
φ	Circumferential coordinate
w	Transverse coordinate and transverse displacement of the deflected membrane
u	Radial displacement of the deflected membrane
u_0	Radial plane displacement
σ_r	Radial stress
σ_t	Circumferential stress
e_r	Radial strain
e_t	Circumferential strain
σ_0	Initial stress
e_0	Initial strain
θ	Slope angle of the deflected membrane
π	Pi (ratio of circumference to diameter)
Q	Dimensionless loads (aq/hE)
W	Dimensionless transverse displacement (w/a)
S_r	Dimensionless radial stress (σ_r/E)
S_t	Dimensionless circumferential stress (σ_t/E)
S_0	Dimensionless initial stress (σ_0/E)
x	Dimensionless radial coordinate (r/a)
b_i	Coefficients of the power-series for S_r
c_i	Coefficients of the power-series for W

Appendix A

$$b_2 = \frac{Q^2}{64{b_0}^2(vb_0 - b_0 - 1)},$$

$$b_4 = \frac{Q^4}{12288{b_0}^5(vb_0 - b_0 - 1)^3}(16v^2{b_0}^3 - 32v{b_0}^3 - 32v{b_0}^2 + 16{b_0}^3 - 5vb_0 + 32{b_0}^2 + 23b_0 + 2),$$

$$\begin{aligned} b_6 = {} & \frac{Q^6}{4718592{b_0}^8(vb_0 - b_0 - 1)^5}(768v^4{b_0}^6 - 3072v^3{b_0}^6 - 3072v^3{b_0}^5 + 4608v^2{b_0}^6 - 448v^3{b_0}^4 + 9216v^2{b_0}^5 - 3072v{b_0}^6 \\ & + 6176v^2{b_0}^4 - 9216v{b_0}^5 + 768{b_0}^6 + 1120v^2{b_0}^3 - 11008v{b_0}^4 + 3072{b_0}^5 + 89v^2{b_0}^2 - 5760v{b_0}^3 + 5280{b_0}^4 - 1176v{b_0}^2 \\ & + 4640{b_0}^3 - 60vb_0 + 2107{b_0}^2 + 316b_0 + 13) \end{aligned},$$

$$\begin{aligned} b_8 = {} & \frac{Q^8}{3019898880{b_0}^{11}(vb_0 - b_0 - 1)^7}(73728v^6{b_0}^9 - 442368v^5{b_0}^9 - 442368v^5{b_0}^8 + 1105920v^4{b_0}^9 - 62208v^5{b_0}^7 \\ & + 2211840v^4{b_0}^8 - 1474560v^3{b_0}^9 + 1452288v^4{b_0}^7 - 4423680v^3{b_0}^8 + 1105920v^2{b_0}^9 + 284160v^4{b_0}^6 - 5187072v^3{b_0}^7 \\ & + 4423680v^2{b_0}^8 - 442368v{b_0}^9 + 22272v^4{b_0}^5 - 2752512v^3{b_0}^6 + 7469568v^2{b_0}^7 - 2211840v{b_0}^8 + 73728{b_0}^9 \\ & - 633504v^3{b_0}^5 + 6552576v^2{b_0}^6 - 4876032v{b_0}^7 + 442368{b_0}^8 - 63008v^3{b_0}^4 + 3094560v^2{b_0}^5 - 5984256v{b_0}^6 \\ & + 1203456{b_0}^7 - 3405v^3{b_0}^3 + 720544v^2{b_0}^4 - 4377696v{b_0}^5 + 1900032{b_0}^6 + 81383v^2{b_0}^3 - 1855328v{b_0}^4 + 1894368{b_0}^5 \\ & + 3046v^2{b_0}^2 - 412839v{b_0}^3 + 1197792{b_0}^4 - 38112v{b_0}^2 + 454741{b_0}^3 - 1131vb_0 + 82802{b_0}^2 + 6521b_0 + 170) \end{aligned},$$

$$b_{10} = \frac{Q^{10}}{2899102924800 b_0{}^{14} (v b_0 - b_0 - 1)^9} (11796480 v^8 b_0{}^{12} - 94371840 v^7 b_0{}^{12} - 94371840 v^7 b_0{}^{11} + 330301440 v^6 b_0{}^{12} - 12976128 v^7 b_0{}^{10} + 660602880 v^6 b_0{}^{11} - 660602880 v^5 b_0{}^{12} + 429146112 v^6 b_0{}^{10} - 1981808640 v^5 b_0{}^{11} + 825753600 v^4 b_0{}^{12} + 85868544 v^6 b_0{}^9 - 2302377984 v^5 b_0{}^{10} + 3303014400 v^4 b_0{}^{11} - 660602880 v^3 b_0{}^{12} + 6505728 v^6 b_0{}^8 - 1223884800 v^5 b_0{}^9 + 5528862720 v^4 b_0{}^{10} - 3303014400 v^3 b_0{}^{11} + 330301440 v^2 b_0{}^{12} - 291371008 v^5 b_0{}^8 + 4831395840 v^4 b_0{}^9 - 7220428800 v^3 b_0{}^{10} + 1981808640 v^2 b_0{}^{11} - 94371840 v b_0{}^{12} - 32214016 v^5 b_0{}^7 + 2308777216 v^4 b_0{}^8 - 8804106240 v^3 b_0{}^9 + 5347196928 v^2 b_0{}^{10} - 660602880 v b_0{}^{11} + 11796480 b_0{}^{12} - 1794592 v^5 b_0{}^6 + 583241728 v^4 b_0{}^7 - 6451513344 v^3 b_0{}^8 + 8374763520 v^2 b_0{}^9 - 2120712192 v b_0{}^{10} + 94371840 b_0{}^{11} + 78875520 v^4 b_0{}^6 - 2845976576 v^3 b_0{}^7 + 8318000896 v^2 b_0{}^8 - 4058578944 v b_0{}^9 + 351289344 b_0{}^{10} + 5520032 v^4 b_0{}^5 - 729447296 v^3 b_0{}^6 + 5360619520 v^2 b_0{}^7 - 5098749952 v b_0{}^8 + 794542080 b_0{}^9 + 226595 v^4 b_0{}^4 - 103846016 v^3 b_0{}^5 + 2205793728 v^2 b_0{}^6 - 4355206144 v b_0{}^7 + 1208350464 b_0{}^8 - 8153804 v^3 b_0{}^4 + 546622400 v^2 b_0{}^5 - 2529774688 v b_0{}^6 + 1289535488 b_0{}^7 - 247276 v^3 b_0{}^3 + 76426626 v^2 b_0{}^4 - 962168448 v b_0{}^5 + 976347328 b_0{}^6 + 5102816 v^2 b_0{}^3 - 221839044 v b_0{}^4 + 513872032 b_0{}^5 + 121893 v^2 b_0{}^2 - 27116356 v b_0{}^3 + 177612267 b_0{}^4 - 1557948 v b_0{}^2 + 35453088 b_0{}^3 - 32012 v b_0 + 3807527 b_0{}^2 + 197432 b_0 + 3700)$$

$$b_{12} = \frac{Q^{12}}{38963943309312000 b_0{}^{17} (v b_0 - b_0 - 1)^{11}} (2831155200 v^{10} b_0{}^{15} - 28311552000 v^9 b_0{}^{15} - 28311552000 v^9 b_0{}^{14} + 127401984000 v^8 b_0{}^{15} - 3833856000 v^9 b_0{}^{13} + 254803968000 v^8 b_0{}^{14} - 3397386240000 v^7 b_0{}^{15} + 1644193382400 v^8 b_0{}^{13} - 1019215872000 v^7 b_0{}^{14} + 594542592000 v^6 b_0{}^{15} + 33183498240 v^8 b_0{}^{12} - 1177335889920 v^7 b_0{}^{13} + 2378170368000 v^6 b_0{}^{14} - 713451110400 v^5 b_0{}^{15} + 2441416704 v^8 b_0{}^{11} - 625307811840 v^7 b_0{}^{12} + 3959653662720 v^6 b_0{}^{13} - 3567255552000 v^5 b_0{}^{14} + 594542592000 v^4 b_0{}^{15} - 150842204160 v^7 b_0{}^{11} + 3448016732160 v^6 b_0{}^{12} - 7758285373440 v^5 b_0{}^{13} + 3567255552000 v^4 b_0{}^{14} - 339738624000 v^3 b_0{}^{15} - 17213718528 v^7 b_0{}^{10} + 1654010339328 v^6 b_0{}^{11} - 9414912245760 v^5 b_0{}^{12} + 9577090252800 v^4 b_0{}^{13} - 2378170368000 v^3 b_0{}^{14} + 127401984000 v^2 b_0{}^{15} - 935561984 v^7 b_0{}^9 + 430454685696 v^6 b_0{}^{10} - 6893095084032 v^5 b_0{}^{11} + 14917238784000 v^4 b_0{}^{12} - 7597263421440 v^3 b_0{}^{13} + 1019215872000 v^2 b_0{}^{14} - 28311552000 v b_0{}^{15} + 61819041536 v^6 b_0{}^9 - 3084866224128 v^5 b_0{}^{10} + 14763898306560 v^4 b_0{}^{11} - 14452669808640 v^3 b_0{}^{12} + 3775628574720 v^2 b_0{}^{13} - 254803968000 v b_0{}^{14} + 2831155200 b_0{}^{15} + 4895263744 v^6 b_0{}^8 - 830821516032 v^5 b_0{}^9 + 9569990983680 v^4 b_0{}^{10} - 18062091362304 v^3 b_0{}^{11} + 8485774295040 v^2 b_0{}^{12} - 1073821777920 v b_0{}^{13} + 28311552000 b_0{}^{14} + 215192016 v^6 b_0{}^7 - 133108374528 v^5 b_0{}^8 + 4054231566080 v^4 b_0{}^9 - 15437915258880 v^3 b_0{}^{10} + 12823006617600 v^2 b_0{}^{11} - 2784346767360 v b_0{}^{12} + 133748490240 b_0{}^{13} - 12875099008 v^5 b_0{}^7 + 1095239501824 v^4 b_0{}^8 - 9112347265280 v^3 b_0{}^9 + 13647129919488 v^2 b_0{}^{10} - 4937554894848 v b_0{}^{11} + 393023324160 b_0{}^{12} - 706597280 v^5 b_0{}^6 + 184425366224 v^4 b_0{}^7 - 3662062729216 v^3 b_0{}^8 + 10412228738304 v^2 b_0{}^9 - 6298378960896 v b_0{}^{10} + 800226865152 b_0{}^{11} - 23265835 v^5 b_0{}^5 + 18873314784 v^4 b_0{}^6 - 970308536704 v^3 b_0{}^7 + 5672405965824 v^2 b_0{}^8 - 5914599680256 v b_0{}^9 + 1190798573568 b_0{}^{10} + 1149972301 v^4 b_0{}^5 - 162363986880 v^3 b_0{}^6 + 2154848417648 v^2 b_0{}^7 - 4103411461120 v b_0{}^8 + 1330424677632 b_0{}^9 + 29723638 v^4 b_0{}^4 - 16413332062 v^3 b_0{}^5 + 545497494080 v^2 b_0{}^6 - 2073388347136 v b_0{}^7 + 1126041833472 b_0{}^8 - 869453064 v^3 b_0{}^4 + 86826403730 v^2 b_0{}^5 - 736239620256 v b_0{}^6 + 717083006960 b_0{}^7 - 17763561 v^3 b_0{}^3 + 7885361588 v^2 b_0{}^4 - 173225183639 v b_0{}^5 + 334939395552 b_0{}^6 + 360240495 v^2 b_0{}^3 - 24839463000 v b_0{}^4 + 109293631105 b_0{}^5 + 6241422 v^2 b_0{}^2 - 2013854207 v b_0{}^3 + 22985307318 b_0{}^4 - 82446808 v b_0{}^2 + 2956637097 b_0{}^3 - 1280564 v b_0 + 219170970 b_0{}^2 + 8330804 b_0 + 120500)$$

$$b_{14} = \frac{1}{112 b_0{}^2 (v b_0 - b_0 - 1)} (21 Q^2 v b_0 b_{12} + 56 Q^2 v b_2 b_{10} + 77 Q^2 v b_4 b_8 + 42 Q^2 v b_6{}^2 - 480 v b_0{}^2 b_2 b_{12} - 576 v b_0{}^2 b_4 b_{10} - 624 v b_0{}^2 b_6 b_8 - 540 v b_0 b_2{}^2 b_{10} - 1152 v b_0 b_2 b_4 b_8 - 588 v b_0 b_2 b_6{}^2 - 576 v b_0 b_4{}^2 b_6 - 180 v b_2{}^3 b_8 - 540 v b_2{}^2 b_4 b_6 - 176 v b_2 b_4{}^3 - 21 Q^2 b_0 b_{12} - 136 Q^2 b_2 b_{10} - 253 Q^2 b_4 b_8 - 150 Q^2 b_6{}^2 + 936 b_0{}^2 b_2 b_{12} + 1656 b_0{}^2 b_4 b_{10} + 2112 b_0{}^2 b_6 b_8 + 1196 b_0 b_2{}^2 b_{10} + 3088 b_0 b_2 b_4 b_8 + 1692 b_0 b_2 b_6{}^2 + 1584 b_0 b_4{}^2 b_6 + 404 b_2{}^3 b_8 + 1316 b_2{}^2 b_4 b_6 + 424 b_2 b_4{}^3 - 21 Q^2 b_{12} + 176 b_0 b_2 b_{12} + 144 b_0 b_4 b_{10} + 128 b_0 b_6 b_8 + 68 b_2{}^2 b_{10} + 112 b_2 b_4 b_8 + 52 b_2 b_6{}^2 + 48 b_4{}^2 b_6)$$

$$b_{16} = \frac{1}{72 b_0{}^2 (v b_0 - b_0 - 1)} (14 Q^2 v b_0 b_{14} + 38 Q^2 v b_2 b_{12} + 54 Q^2 v b_4 b_{10} + 62 Q^2 v b_6 b_8 - 314 v b_0{}^2 b_2 b_{14} - 384 v b_0{}^2 b_4 b_{12} - 426 v b_0{}^2 b_6 b_{10} - 220 v b_0{}^2 b_8{}^2 - 362 v b_0 b_2{}^2 b_{12} - 788 v b_0 b_2 b_4 b_{10} - 820 v b_0 b_2 b_6 b_8 - 400 v b_0 b_4{}^2 b_8 - 402 v b_0 b_4 b_6{}^2 - 124 v b_2{}^3 b_{10} - 378 v b_2{}^2 b_4 b_8 - 190 v b_2{}^2 b_6{}^2 - 370 v b_2 b_4{}^2 b_6 - 30 v b_4{}^4 - 14 Q^2 b_0 b_{14} - 95 Q^2 b_2 b_{12} - 189 Q^2 b_4 b_{10} - 248 Q^2 b_6 b_8 + 622 b_0{}^2 b_2 b_{14} + 1152 b_0{}^2 b_4 b_{12} + 1566 b_0{}^2 b_6 b_{10} + 860 b_0{}^2 b_8{}^2 + 826 b_0 b_2{}^2 b_{12} + 2244 b_0 b_2 b_4 b_{10} + 2636 b_0 b_2 b_6 b_8 + 1200 b_0 b_4{}^2 b_8 + 1242 b_0 b_4 b_6{}^2 + 292 b_2{}^3 b_{10} + 1002 b_2{}^2 b_4 b_8 + 530 b_2{}^2 b_6{}^2 + 990 b_2 b_4{}^2 b_6 + 78 b_4{}^4 - 14 Q^2 b_{14} + 116 b_0 b_2 b_{14} + 96 b_0 b_4 b_{12} + 84 b_0 b_6 b_{10} + 40 b_0 b_8{}^2 + 46 b_2{}^2 b_{12} + 76 b_2 b_4 b_{10} + 68 b_2 b_6 b_8 + 32 b_4{}^2 b_8 + 30 b_4 b_6)$$

$$b_{18} = \frac{1}{180 b_0{}^2 (v b_0 - b_0 - 1)} (36 Q^2 v b_0 b_{16} + 99 Q^2 v b_2 b_{14} + 144 Q^2 v b_4 b_{12} + 171 Q^2 v b_6 b_{10} + 90 Q^2 v b_8{}^2 - 796 v b_0{}^2 b_2 b_{16} - 988 v b_0{}^2 b_4 b_{14} - 1116 v b_0{}^2 b_6 b_{12} - 1180 v b_0{}^2 b_8 b_{10} - 936 v b_0 b_2{}^2 b_{14} - 2072 v b_0 b_2 b_4 b_{12} - 2192 v b_0 b_2 b_6 b_{10} - 1116 v b_0 b_2 b_8{}^2 - 1068 v b_0 b_4{}^2 b_{10} - 2168 v b_0 b_4 b_6 b_8 - 360 v b_0 b_6{}^3 - 328 v b_2{}^3 b_{12} - 1016 v b_2{}^2 b_4 b_{10} - 1032 v b_2{}^2 b_6 b_8 - 1004 v b_2 b_4{}^2 b_8 - 1000 v b_2 b_4 b_6{}^2 - 324 v b_4{}^3 b_6 - 36 Q^2 b_0 b_{16} - 253 Q^2 b_2 b_{14} - 528 Q^2 b_4 b_{12} - 741 Q^2 b_6 b_{10} - 410 Q^2 b_8{}^2 + 1596 b_0{}^2 b_2 b_{16} + 3060 b_0{}^2 b_4 b_{14} + 4356 b_0{}^2 b_6 b_{12} + 5100 b_0{}^2 b_8 b_{10} + 2184 b_0 b_2{}^2 b_{14} + 6168 b_0 b_2 b_4 b_{12} + 7632 b_0 b_2 b_6 b_{10} + 4092 b_0 b_2 b_8{}^2 + 3420 b_0 b_4{}^2 b_{10} + 7368 b_0 b_4 b_6 b_8 + 1224 b_0 b_6{}^3 + 800 b_2{}^3 b_{12} + 2864 b_2{}^2 b_4 b_{10} + 3192 b_2{}^2 b_6 b_8 + 2924 b_2 b_4{}^2 b_8 + 2976 b_2 b_4 b_6{}^2 + 924 b_4{}^3 b_6 - 36 Q^2 b_{16} + 296 b_0 b_2 b_{16} + 248 b_0 b_4 b_{14} + 216 b_0 b_6 b_{12} + 200 b_0 b_8 b_{10} + 120 b_2{}^2 b_{14} + 200 b_2 b_4 b_{12} + 176 b_2 b_6 b_{10} + 84 b_2 b_8{}^2 + 84 b_4{}^2 b_{10} + 152 b_4 b_6 b_8 + 24 b_6{}^3)$$

$$b_{20} = \frac{1}{220b_0{}^2(vb_0-b_0-1)}(45Q^2vb_0b_{18}+125Q^2vb_2b_{16}+185Q^2vb_4b_{14}+225Q^2vb_6b_{12}+245Q^2vb_8b_{10}-984vb_0{}^2b_2b_{18}$$
$$-1236vb_0{}^2b_4b_{16}-1416vb_0{}^2b_6b_{14}-1524vb_0{}^2b_8b_{12}-780vb_0{}^2b_{10}{}^2-1176vb_0b_2{}^2b_{16}-2640vb_0b_2b_4b_{14}-2832vb_0b_2b_6b_{12}$$
$$-2928vb_0b_2b_8b_{10}-1380vb_0b_4{}^2b_{12}-2832vb_0b_4b_6b_{10}-1428vb_0b_4b_8{}^2-1416vb_0b_6{}^2b_8-420vb_2{}^3b_{14}-1320vb_2{}^2b_4b_{12}$$
$$-1356vb_2{}^2b_6b_{10}-684vb_2{}^2b_8{}^2-1320vb_2b_4{}^2b_{10}-2640vb_2b_4b_6b_8-436vb_2b_6{}^3-428vb_4{}^3b_8-636vb_4{}^2b_6{}^2-45Q^2b_0b_{18}$$
$$-325Q^2b_2b_{16}-703Q^2b_4b_{14}-1035Q^2b_6b_{12}-1225Q^2b_8b_{10}+1992b_0{}^2b_2b_{18}+3924b_0{}^2b_4b_{16}+5784b_0{}^2b_6b_{14}+7092b_0{}^2b_8b_{12}$$
$$+3780b_0{}^2b_{10}{}^2+2792b_0b_2{}^2b_{16}+8128b_0b_2b_4b_{14}+10464b_0b_2b_6b_{12}+11824b_0b_2b_8b_{10}+4644b_0b_4{}^2b_{12}+10368b_0b_4b_6b_{10}$$
$$+5396b_0b_4b_8{}^2+5256b_0b_6{}^2b_8+1052b_2{}^3b_{14}+3896b_2{}^2b_4b_{12}+4532b_2{}^2b_6b_{10}+2388b_2{}^2b_8{}^2+4104b_2b_4{}^2b_{10}+8608b_2b_4b_6b_8$$
$$+1420b_2b_6{}^3+1324b_4{}^3b_8+1980b_4{}^2b_6{}^2-45Q^2b_{18}+368b_0b_2b_{18}+312b_0b_4b_{16}+272b_0b_6b_{14}+248b_0b_8b_{12}+120b_0b_{10}{}^2$$
$$+152b_2{}^2b_{16}+256b_2b_4b_{14}+224b_2b_6b_{12}+208b_2b_8b_{10}+108b_4{}^2b_{12}+192b_4b_6b_{10}+92b_4b_8{}^2+88b_6{}^2b_8)$$

Appendix B

$$c_2 = -\frac{1}{4}\frac{Q}{b_0},$$

$$c_4 = -\frac{Q}{64b_0^3}(Q^2-8b_0b_2),$$

$$c_6 = -\frac{Q}{1536b_0^5}(3Q^4-48Q^2b_0b_2-128b_0^3b_4+128b_0^2b_2^2),$$

$$c_8 = -\frac{Q}{16384b_0^7}(5Q^6-120Q^4b_0b_2-384Q^2b_0^3b_4+768Q^2b_0^2b_2^2-1024b_0^5b_6+2048b_0^4b_2b_4-1024b_0^3b_2^3),$$

$$c_{10} = -\frac{Q}{655360b_0^9}(35Q^8-1120Q^6b_0b_2-3840Q^4b_0^3b_4+11520Q^4b_0^2b_2^2-12288Q^2b_0^5b_6+49152Q^2b_0^4b_2b_4-40960Q^2b_0^3b_2^3$$
$$-32768b_0^7b_8+65536b_0^6b_2b_6+32768b_0^6b_4^2-98304b_0^5b_2^2b_4+32768b_0^4b_2^4),$$

$$c_{12} = -\frac{Q}{6291456b_0^{11}}(63Q^{10}-2520Q^8b_0b_2-8960Q^6b_0^3b_4+35840Q^6b_0^2b_2^2-30720Q^4b_0^5b_6-215040Q^4b_0^3b_2^3$$
$$-98304Q^2b_0^7b_8+196608Q^2b_0^6b_2^4+393216Q^2b_0^6b_2b_6+491520Q^2b_0^4b_2^4-983040Q^2b_0^5b_2^2b_4+184320Q^2b_0^4b_2b_4$$
$$-262144b_0^9b_{10}+524288b_0^8b_2b_8+524288b_0^8b_4b_6-786432b_0^7b_2^2b_6-786432b_0^7b_2b_4^2+1048576b_0^6b_2^4b_4-262144b_0^5b_2^5),$$

$$c_{14} = -\frac{Q}{117440512b_0^{13}}(231Q^{12}-11088Q^{10}b_0b_6-40320Q^8b_0^3b_4+201600Q^8b_0^2b_2^2-143360Q^6b_0^5b_6+1146880Q^6b_0^4b_2b_4$$
$$-1720320Q^6b_0^3b_2^3-491520Q^4b_0^7b_8+2949120Q^4b_0^6b_2b_6+1474560Q^4b_0^6b_4^2-10321920Q^4b_0^5b_2^2b_4+6881280Q^4b_0^4b_2^4$$
$$-1572864Q^2b_0^9b_{10}+6291456Q^2b_0^8b_2b_8+6291456Q^2b_0^8b_4b_6-15728640Q^2b_0^7b_2b_4^2-15728640Q^2b_0^7b_2^2b_6+4194304b_0^6b_2^6,$$
$$+31457280Q^2b_0^6b_2^3b_4-11010048Q^2b_0^5b_2^5+8388608b_0^{10}b_2b_{10}+8388608b_0^{10}b_4b_8-4194304b_0^{11}b_{12}+4194304b_0^{10}b_6^2$$
$$-12582912b_0^9b_2^2b_8-4194304b_0^9b_4^3-25165824b_0^9b_2b_4b_6+25165824b_0^8b_2^2b_4^2+16777216b_0^8b_2^3b_6-20971520b_0^7b_2^4b_4),$$

$$c_{16} = -\frac{Q}{1073741824b_0^{15}}(429Q^{14}-24024Q^{12}b_0b_2-88704Q^{10}b_0^3b_4-322560Q^8b_0^5b_6+3225600Q^8b_0^4b_2b_4$$
$$+9175040Q^6b_0^6b_2b_6-41287680Q^6b_0^5b_2^2b_4+34406400Q^6b_0^4b_2^4-3932160Q^4b_0^9b_{10}+23592960Q^4b_0^8b_2b_8$$
$$+23590960Q^4b_0^8b_4b_6-82575360Q^4b_0^7b_2b_4^2+220200960Q^4b_0^6b_2^3b_4-99090432Q^4b_0^5b_2^5-12582912Q^2b_0^{11}b_{12}$$
$$+50331648Q^2b_0^{10}b_2b_{10}+50331648Q^2b_0^{10}b_4b_8+25165824Q^2b_0^{10}b-125829120Q^2b_0^9b_2^2b_8-251658240Q^2b_0^9b_2b_4b_6,$$
$$-41943040Q^2b_0^9b_4^3+377487360Q^2b_0^8b_2^2b_4^2+251658240Q^2b_0^8b_2^3b_6-440401920Q^2b_0^7b_2^4b_4+117440512Q^2b_0^6b_2^6$$
$$-33554432b_0^{13}b_{14}+67108864b_0^{12}b_2b_{12}+67108864b_0^{12}b_4b_{10}+67108864b_0^{12}b_6b_8-100663296b_0^{11}b_2^2b_{10}$$
$$-201326592b_0^{11}b_2b_4b_8-100663296b_0^{11}b_2b_6^2-100663296b_0^{11}b_4^2b_6+134217728b_0^{10}b_2^3b_8+402653184b_0^{10}b_2^2b_4b_6$$
$$+134217728b_0^{10}b_2b_4^3-167772160b_0^9b_2^4b_6-335544320b_0^9b_2^3b_4^2+201326592b_0^8b_2^5b_4-33554432b_0^7b_2^7)$$

$$
\begin{aligned}
c_{18} \;=\; & -\tfrac{1}{77309411328{b_0}^{17}}Q(6435Q^{16} - 411840Q^{14}b_0b_2 - 1537536Q^{12}{b_0}^3b_4 + 10762752Q^{12}{b_0}^2{b_2}^2 - 5677056Q^{10}{b_0}^5b_6 \\
& +68124672Q^{10}{b_0}^4b_2b_4 - 147603456Q^{10}{b_0}^3{b_2}^3 - 20643840Q^8{b_0}^7b_8 + 206438400Q^8{b_0}^6b_2b_6 + 103219200Q^8{b_0}^6{b_4}^2 \\
& -1135411200Q^8{b_0}^5{b_2}^2b_4 + 1135411200Q^8{b_0}^4{b_2}^4 - 73400320Q^6{b_0}^9b_{10} + 587202560Q^6{b_0}^8b_2b_8 + 587202560Q^6{b_0}^8b_4b_6 \\
& -2642411520Q^6{b_0}^7{b_2}^2b_6 - 2642411520Q^6{b_0}^7b_2{b_4}^2 + 8808038400Q^6{b_0}^6{b_2}^3b_4 - 4844421120Q^6{b_0}^5{b_2}^5 \\
& -251658240Q^4{b_0}^{11}b_{12} + 1509949440Q^4{b_0}^{10}b_2b_{10} + 1509949440Q^4{b_0}^{10}b_4b_8 + 754974720Q^4{b_0}^{10}{b_6}^2 \\
& -5284823040Q^4{b_0}^9{b_2}^2b_8 - 10569646080Q^4{b_0}^9b_2b_4b_6 - 1761607680Q^4{b_0}^9{b_4}^3 + 14092861440Q^4{b_0}^8{b_2}^3b_6 \\
& +21139292160Q^4{b_0}^8{b_2}^2{b_4}^2 - 31708938240Q^4{b_0}^7{b_2}^4b_4 + 10569646080Q^4{b_0}^6{b_2}^6 - 805306368Q^2{b_0}^{13}b_{14} \\
& +3221225472Q^2{b_0}^{12}b_2b_{12} + 3221225472Q^2{b_0}^{12}b_4b_{10} + 3221225472Q^2{b_0}^{12}b_6b_8 - 8053063680Q^2{b_0}^{11}{b_2}^2b_{10} \\
& -16106127360Q^2{b_0}^{11}b_2b_4b_8 - 8053063680Q^2{b_0}^{11}b_2{b_6}^2 - 8053063680Q^2{b_0}^{11}{b_4}^2b_6 + 16106127360Q^2{b_0}^{10}{b_2}^3b_8 \\
& +48318382080Q^2{b_0}^{10}{b_2}^2b_4b_6 + 16106127360Q^2{b_0}^{10}b_2{b_4}^3 - 28185722880Q^2{b_0}^9{b_2}^4b_6 - 56371445760Q^2{b_0}^9{b_2}^3{b_4}^2 \\
& +45097156608Q^2{b_0}^8{b_2}^5b_4 - 9663676416Q^2{b_0}^7{b_2}^7 - 2147483648{b_0}^{15}b_{16} + 4294967296{b_0}^{14}b_2b_{14} \\
& +4294967296{b_0}^{14}b_4b_{12} + 4294967296{b_0}^{14}b_6b_{10} + 2147483648{b_0}^{14}{b_8}^2 - 6442450944{b_0}^{13}{b_2}^2b_{12} \\
& -12884901888{b_0}^{13}b_2b_4b_{10} - 12884901888{b_0}^{13}b_2b_6b_8 - 6442450944{b_0}^{13}{b_4}^2b_8 - 6442450944{b_0}^{13}b_4{b_6}^2 \\
& +8589934592{b_0}^{12}{b_2}^3b_{10} + 25769803776{b_0}^{12}{b_2}^2b_4b_8 + 12884901888{b_0}^{12}{b_2}^2{b_6}^2 + 25769803776{b_0}^{12}b_2{b_4}^2b_6 \\
& +2147483648{b_0}^{12}{b_4}^4 - 10737418240{b_0}^{11}b_2{b_4}^2b_8 - 42949672960{b_0}^{11}{b_2}^3b_4b_6 - 21474836480{b_0}^{11}{b_2}^2{b_4}^3 \\
& +12884901888{b_0}^{10}{b_2}^5b_6 + 32212254720{b_0}^{10}{b_2}^4{b_4}^2 - 15032385536{b_0}^9{b_2}^6b_4 + 2147483648{b_0}^8{b_2}^8)
\end{aligned}
$$

$$
\begin{aligned}
c_{20} \;=\; & -\tfrac{1}{687194767360{b_0}^{19}}Q(12155Q^{18} - 875160Q^{16}b_0b_2 - 3294720Q^{14}{b_0}^3b_4 + 26357760Q^{14}{b_0}^2{b_2}^2 \\
& -12300288Q^{12}{b_0}^5b_6 + 172204032Q^{12}{b_0}^4b_2b_4 - 430510080Q^{12}{b_0}^3{b_2}^3 - 45416448Q^{10}{b_0}^7b_8 + 544997376Q^{10}{b_0}^6b_2b_6 \\
& +272498688Q^{10}{b_0}^6{b_4}^2 - 3542482944Q^{10}{b_0}^5{b_2}^2b_4 + 4132896768Q^{10}{b_0}^4{b_2}^4 - 165150720Q^8{b_0}^9b_{10} \\
& +1651507200Q^8{b_0}^8b_2b_8 + 1651507200Q^8{b_0}^8b_4b_6 - 9083289600Q^8{b_0}^7{b_2}^2b_6 - 9083289600Q^8{b_0}^7b_2{b_4}^2 \\
& +36333158400Q^8{b_0}^6{b_2}^3b_4 - 23616552960Q^8{b_0}^5{b_2}^5 - 587202560Q^6{b_0}^{11}b_{12} + 4697620480Q^6{b_0}^{10}b_2b_{10} \\
& +4697620480Q^6{b_0}^{10}b_4b_8 + 2348810240Q^6{b_0}^{10}{b_6}^2 - 21139292160Q^6{b_0}^9{b_2}^2b_8 - 42278584320Q^6{b_0}^9b_2b_4b_6 \\
& -7046430720Q^6{b_0}^9{b_4}^3 + 70464307200Q^6{b_0}^8{b_2}^3b_6 + 105696460800Q^6{b_0}^8b_2{b_4}^2 - 193776844800Q^6{b_0}^7{b_2}^4b_4 \\
& +77510737920Q^6{b_0}^6{b_2}^6 - 201326592OQ^4{b_0}^{13}b_{14} + 12079595520Q^4{b_0}^{12}b_2b_{12} + 12079595520Q^4{b_0}^{12}b_4b_{10} \\
& +12079595520Q^4{b_0}^{12}b_6b_8 - 42278584320Q^4{b_0}^{11}{b_2}^2b_{10} - 84557168640Q^4{b_0}^{11}b_2b_4b_8 - 42278584320Q^4{b_0}^{11}b_2{b_6}^2 \\
& -42278584320Q^4{b_0}^{11}{b_4}^2b_6 + 112742891520Q^4{b_0}^{10}{b_2}^3b_8 + 338228674560Q^4{b_0}^{10}{b_2}^2b_4b_6 + 112742891520Q^4{b_0}^{10}b_2{b_4}^3 \\
& -253671505920Q^4{b_0}^9{b_2}^4b_6 - 507343011840Q^4{b_0}^9{b_2}^3{b_4}^2 + 507343011840Q^4{b_0}^8{b_2}^5b_4 - 132875550720Q^4{b_0}^7{b_2}^7 \\
& -6442450944Q^2{b_0}^{15}b_{16} + 25769803776Q^2{b_0}^{14}b_2b_{14} + 25769803776Q^2{b_0}^{14}b_4b_{12} + 25769803776Q^2{b_0}^{14}b_6b_{10} \\
& +12884901888Q^2{b_0}^{14}{b_8}^2 - 64424509440Q^2{b_0}^{13}{b_2}^2b_{12} - 128849018880Q^2{b_0}^{13}b_2b_4b_{10} - 128849018880Q^2{b_0}^{13}b_2b_6b_8 \\
& -64424509440Q^2{b_0}^{13}{b_4}^2b_8 - 64424509440Q^2{b_0}^{13}b_4{b_6}^2 + 128849018880Q^2{b_0}^{12}{b_2}^3b_{10} + 386547056640Q^2{b_0}^{12}{b_2}^2b_4b_8 \\
& +193273528320Q^2{b_0}^{12}{b_2}^2{b_6}^2 + 386547056640Q^2{b_0}^{12}b_2{b_4}^2b_6 + 32212254720Q^2{b_0}^{12}{b_4}^4 - 225485783040Q^2{b_0}^{11}b_2{b_4}^3 \\
& -901943132160Q^2{b_0}^{11}{b_2}^3b_4b_6 - 450971566080Q^2{b_0}^{11}{b_2}^2{b_4}^3 + 360777252864Q^2{b_0}^{10}{b_2}^5b_6 + 901943132160Q^2{b_0}^{10}{b_2}^4{b_4}^2 \\
& -541165879296Q^2{b_0}^9{b_2}^6b_4 + 96636764160Q^2{b_0}^8{b_2}^8 - 17179869184{b_0}^{17}b_{18} + 34359738368{b_0}^{16}b_2b_{16} \\
& +34359738368{b_0}^{16}b_4b_{14} + 34359738368{b_0}^{16}b_6b_{12} + 34359738368{b_0}^{16}b_8b_{10} - 51539607552{b_0}^{15}{b_2}^2b_{14} \\
& -103079215104{b_0}^{15}b_2b_4b_{12} - 103079215104{b_0}^{15}b_2b_6b_{10} - 51539607552{b_0}^{15}b_2{b_8}^2 - 51539607552{b_0}^{15}{b_4}^2b_{10} \\
& -103079215104{b_0}^{15}b_4b_6b_8 - 17179869184{b_0}^{15}{b_6}^3 + 68719476736{b_0}^{14}{b_2}^3b_{12} + 206158430208{b_0}^{14}{b_2}^2b_4b_{10} \\
& +206158430208{b_0}^{14}{b_2}^2b_6b_8 + 206158430208{b_0}^{14}b_2{b_4}^2b_8 + 206158430208{b_0}^{14}b_2b_4{b_6}^2 + 68719476736{b_0}^{14}{b_4}^3b_6 \\
& -85899345920{b_0}^{13}{b_2}^4b_{10} - 343597383680{b_0}^{13}{b_2}^3b_4b_8 - 171798691840{b_0}^{13}{b_2}^3{b_6}^2 - 515396075520{b_0}^{13}{b_2}^2{b_4}^2b_6 \\
& -85899345920{b_0}^{13}b_2{b_4}^4 + 103079215104{b_0}^{12}{b_2}^5b_8 + 515396075520{b_0}^{12}{b_2}^4b_4b_6 + 343597383680{b_0}^{12}{b_2}^3{b_4}^3 \\
& -120259084288{b_0}^{11}{b_2}^6b_6 - 360777252864{b_0}^{11}{b_2}^5{b_4}^2 + 137438953472{b_0}^{10}{b_2}^7b_4 - 17179869184{b_0}^9{b_2}^9)
\end{aligned}
$$

References

1. Le, N.T.; Wang, J.-W.; Wang, C.-C.; Nguyen, T.N. Automatic defect inspection for coated eyeglass based on symmetrized energy analysis of color channels. *Symmetry* **2019**, *11*, 1518. [CrossRef]
2. Li, J.; Wang, R.; Tian, H.; Wang, Y.; Qi, D. Research on the gradual process of the metallization structures and mechanical properties of wood veneer. *Symmetry* **2018**, *10*, 550. [CrossRef]
3. Rehman, A.; Salleh, Z.; Gul, T.; Zaheer, Z. The impact of viscous dissipation on the thin film unsteady flow of GO-EG/GO-W nanofluids. *Mathematics* **2019**, *7*, 653. [CrossRef]
4. Barba, P.D.; Fattorusso, L.; Versaci, M. A 2D non-linear second-order differential model for electrostatic circular membrane MEMS devices: A result of existence and uniqueness. *Mathematics* **2019**, *7*, 1193. [CrossRef]
5. Hencky, H. On the stress state in circular plates with vanishing bending stiffness. *Z. Für Math. Und Phys.* **1915**, *63*, 311–317. (In German)
6. Fernando, M.; Kinloch, A.J. Use of the inverted-blister test to study the adhesion of photopolymers. *Int. J. Adhes. Adhes.* **1990**, *10*, 69–76. [CrossRef]
7. Jensen, H.M.; Thouless, M.D. Effects of residual-stresses in the blister test. *Int. J. Solids Struct.* **1993**, *30*, 779–795. [CrossRef]
8. Lai, Y.H.; Dillard, D.A. A study of the fracture efficiency parameter of blister tests for films and coatings. *J. Adhes. Sci. Technol.* **1994**, *8*, 663–678. [CrossRef]

9. Wan, K.T.; Guo, S.; Dillard, D.A. A theoretical and numerical study of a thin clamped circular film under an external load in the presence of a tensile residual stress. *Thin Solid Film.* **2003**, *425*, 150–162. [CrossRef]
10. Sun, Z.; Wan, K.T.; Dillard, D.A. A theoretical and numerical study of thin film delamination using the pull-off test. *Int. J. Solids Struct.* **2004**, *41*, 717–730. [CrossRef]
11. Guo, S.; Wan, K.T.; Dillard, D.A. A bending-to-stretching analysis of the blister test in the presence of tensile residual stress. *Int. J. Solids Struct.* **2005**, *42*, 2771–2784. [CrossRef]
12. Fichter, W.B. Some solutions for the large deflections of uniformly loaded circular membranes. *NASA Technical Paper No. 3658* **1997**.
13. Jenkins, C.H.; Faisal, S.M. Thermal load effects on precision membranes. *J. Spacecr. Rocket.* **2001**, *38*, 207–211. [CrossRef]
14. Williams, J.G. Energy release rates for the peeling of flexible membranes and the analysis of blister tests. *Int. J. Fract.* **1997**, *87*, 265–288. [CrossRef]
15. Noyan, I.C.; Cohen, J.B. *Residual Stress Measurement by Diffraction and Interpretation*; Springer: New York, NY, USA, 1987.
16. Malhotra, S.G.; Rek, Z.U.; Yalisove, S.M.; Bilello, J.C. Strain gradients and normal stresses in textured Mo thin films. *J. Vac. Sci. Technol. A Vac. Surf. Film.* **1997**, *15*, 345–352. [CrossRef]
17. Tao, J.; Lee, L.H.; Bilello, J.C. Non-destructive evaluation of residual stresses in thin films via x-ray diffraction topography methods. *J. Electron. Mater.* **1991**, *20*, 819–825. [CrossRef]
18. Geisz, J.F.; Kuech, T.F.; Lagally, M.G.; Cardone, F.; Potemski, R.M. Film stress of sputtered W/C multilayers and strain relaxation upon annealing. *J. Appl. Phys.* **1994**, *75*, 1530–1533. [CrossRef]
19. Maden, M.A.; Jagota, A.; Mazur, S.; Farris, R.J. Vibrational technique for stress measurement in films: I, Ideal membrane behavior. *J. Am. Ceram. Soc.* **1994**, *77*, 625–635. [CrossRef]
20. Tong, Q.K.; Maden, M.A.; Jagota, A.; Farris, R.J. Vibrational technique for stress measurement in films: II, Extensions and complicating effects. *J. Am. Ceram. Soc.* **1994**, *77*, 636–648. [CrossRef]
21. Dannenberg, H. Measurement of adhesion by a blister method. *J. Appl. Polym. Sci.* **1961**, *5*, 125–134. [CrossRef]
22. Williams, M.L. Relation of continuum mechanics to adhesive fracture. *J. Adhes.* **1972**, *4*, 307–332. [CrossRef]
23. Beams, J.W. Mechnical properties of thin films of gold and silver. In *Structure and Properties of Thin Films*; proceedings; Neugebauer, C.A., Ed.; Wiley: New York, NY, USA, 1959.
24. Zheng, D.; Xu, Y.; Tsai, Y.P.; Tu, K.N.; Patterson, P.; Zhao, B.; Liu, Q.Z.; Brongo, M. Mechanical property measurement of thin polymeric-low dielectric-constant films using bulge testing method. *Appl. Phys. Lett.* **2000**, *76*, 2008–2010. [CrossRef]
25. Xu, D.; Liechti, K.M. Bulge testing transparent thin films with moiré deflectometry. *Exp. Mech.* **2010**, *50*, 217–225. [CrossRef]
26. Sun, J.Y.; Hu, J.L.; Zheng, Z.L.; He, X.T.; Geng, H.H. A practical method for simultaneous determination of Poisson's ratio and Young's modulus of elasticity of thin films. *J. Mech. Sci. Technol.* **2011**, *25*, 3165–3171. [CrossRef]
27. Sun, J.Y.; Qian, S.H.; Li, Y.M.; He, X.T.; Zheng, Z.L. Theoretical study of adhesion energy measurement for film/substrate interface using pressurized blister test: Energy release rate. *Measurement* **2013**, *46*, 2278–2287. [CrossRef]
28. Xu, D.; Liechti, K.M. Analytical and experimental study of a circular membrane in Hertzian contact with a rigid substrate. *Int. J. Solids Struct.* **2010**, *47*, 207–214. [CrossRef]
29. Chien, W.Z. Asymptotic behavior of a thin clamped circular plate under uniform normal pressure at very large deflection. *Sci. Rep. Natl. Tsinghua Univ.* **1948**, *5*, 193–208.
30. Alekseev, S.A. Elastic circular membranes under the uniformly distributed loads. *Eng. Corpus.* **1953**, *14*, 196–198. (In Russian)
31. Chien, W.Z.; Wang, Z.Z.; Xu, Y.G.; Chen, S.L. The symmetrical deformation of circular membrane under the action of uniformly distributed loads in its portion. *Appl. Math. Mech. (Engl. Ed.)* **1981**, *2*, 653–668.
32. Chien, W.Z.; Chen, S.L. The solution of large deflection problem of thin circular plate by the method of composite expansion. *Appl. Math. Mech. (Engl. Ed.)* **1985**, *6*, 103–118.
33. Arthurs, A.M.; Clegg, J. On the solution of a boundary value problem for the nonlinear Föppl-Hencky equation. *Z. Angew. Math. Mech.* **1994**, *74*, 281–284. [CrossRef]
34. Plaut, R.H. Linearly elastic annular and circular membranes under radial, transverse, and torsional loading. Part I: Large unwrinkled axisymmetric deformations. *Acta Mech.* **2009**, *202*, 79–99. [CrossRef]

35. Lian, Y.S.; He, X.T.; Liu, G.H.; Sun, J.Y.; Zheng, Z.L. Application of perturbation idea to well-known Hencky problem: A perturbation solution without small-rotation-angle assumption. *Mech. Res. Commun.* **2017**, *83*, 32–46. [CrossRef]
36. Sun, J.Y.; Rong, Y.; He, X.T.; Gao, X.W.; Zheng, Z.L. Power series solution of circular membrane under uniformly distributed loads: Investigation into Hencky transformation. *Struct. Eng. Mech.* **2013**, *45*, 631–641. [CrossRef]
37. Yang, Z.X.; Sun, J.Y.; Ran, G.M.; He, X.T. A new solution to Föppl-Hencky membrane equation. *J. Mech.* **2017**, *33*, N7–N11. [CrossRef]
38. Lian, Y.S.; Sun, J.Y.; Yang, Z.X.; He, X.T.; Zheng, Z.L. Closed-form solution of well-known Hencky problem without small-rotation-angle assumption. *Z. Angew. Math. Mech.* **2016**, *96*, 1434–1441. [CrossRef]
39. Lian, Y.S.; Sun, J.Y.; Zhao, Z.H.; He, X.T.; Zheng, Z.L. A revisit of the boundary value problem for Föppl–Hencky membranes: Improvement of geometric equations. *Mathematics* **2020**, *8*, 631. [CrossRef]
40. Ku, C.L. On the large deflection of elastic circular membrane with initial tension under uniformly distributed load. *Chin. J. Phys.* **1956**, *12*, 319–338. (In Chinese)
41. He, X.T.; Wu, J.L.; Zheng, Z.L.; Chen, S.L. Axisymmetrical deformation of prestressed circular membrane under uniformly distributed loads. *J. Chongqing Univ.* **2010**, *33*, 109–112. (In Chinese)
42. Sun, J.Y.; Lian, Y.S.; Li, Y.M.; He, X.T.; Zheng, Z.L. Closed-form solution of elastic circular membrane with initial stress under uniformly-distributed loads: Extended Hencky solution. *Z. Angew. Math. Mech.* **2015**, *95*, 1335–1341. [CrossRef]
43. Yang, Z.X.; Sun, J.Y.; Li, K.; Lian, Y.S.; He, X.T.; Zheng, Z.L. Theoretical study on synchronous characterization of surface and interfacial mechanical properties of thin-film/substrate systems with residual stress based on pressure blister test technique. *Polymers* **2018**, *10*, 49. [CrossRef] [PubMed]
44. Lian, Y.S.; Sun, J.Y.; Dong, J.; Zheng, Z.L.; Yang, Z.X. Closed-form solution of axisymmetric deformation of prestressed Föppl-Hencky membrane under constrained deflecting. *Struct. Eng. Mech.* **2019**, *69*, 693–698.